

# Unifying Dirac Spin Liquids on Square and Shastry–Sutherland Lattices via Fermionic Deconfined Criticality

Andreas Feuerpfeil  <sup>1,2,\*</sup>, Leyna Shackleton  <sup>3</sup>, Atanu Maity  <sup>1</sup>, Ronny Thomale  <sup>1,4</sup>, Subir Sachdev  <sup>5,2</sup> and Yasir Iqbal  <sup>4,†</sup>

<sup>1</sup>Institut für Theoretische Physik und Astrophysik and Würzburg-Dresden Cluster of Excellence ct.qmat, Universität Würzburg, 97074 Würzburg, Germany

<sup>2</sup>Center for Computational Quantum Physics, Flatiron Institute, 162 5th Avenue, New York, NY 10010, USA

<sup>3</sup>Department of Physics, Massachusetts Institute of Technology, Cambridge, Massachusetts 02139, USA

<sup>4</sup>Department of Physics, Indian Institute of Technology Madras, Chennai 600036, India

<sup>5</sup>Department of Physics, Harvard University, Cambridge MA 02138, USA

\* [andreas.feuerpfeil@uni-wuerzburg.de](mailto:andreas.feuerpfeil@uni-wuerzburg.de), † [yiqbal@physics.iitm.ac.in](mailto:yiqbal@physics.iitm.ac.in)

## Abstract

We present a fermionic gauge theory for deconfined quantum criticality on the Shastry–Sutherland lattice and reveal its shared low-energy field-theoretic structure with the square lattice. Starting from an  $SU(2)$   $\pi$ -flux parent state, we construct a continuum theory of Dirac spinons coupled to an  $SU(2)$  gauge field and adjoint Higgs fields whose condensates drive transitions to a staggered-flux  $U(1)$  spin liquid and a gapless  $\mathbb{Z}_2$  Dirac spin liquid. While the Shastry–Sutherland lattice permits additional symmetry-allowed fermion bilinears compared to the square lattice, the quantum field theories are identical up to additional irrelevant terms. Consequently, the Higgs potential structure and the leading low-energy theory coincide with the square-lattice case at the quantum critical point. The  $SO(5)$  critical point is expected to realize conformal deconfined criticality: we analyze it in a large flavor expansion, calculate its critical exponents, and identify the Yukawa coupling between the fermions and Higgs fields as the relevant perturbation that destabilizes it, consistent with pseudocritical behavior observed in recent Monte Carlo studies. We show that the emergent  $SO(5)$  order parameter acquires a large anomalous dimension at the critical point, leading to strongly enhanced Néel and VBS susceptibilities—a hallmark of fermionic deconfined quantum criticality consistent with numerical studies. Our results place recent numerical evidence for a gapless  $\mathbb{Z}_2$  Dirac spin liquid on the Shastry–Sutherland lattice within a controlled field-theoretic framework and demonstrate that fermionic deconfined criticality on the square lattice—including critical exponents and stability—extends to frustrated lattices with reduced symmetry.

Copyright attribution to authors.

This work is a submission to SciPost Physics.

License information to appear upon publication.

Publication information to appear upon publication.

Received Date

Accepted Date

Published Date

## Contents

### 1 Gapless $\mathbb{Z}_2$ spin liquid on the Shastry–Sutherland lattice

4

---

<b>2 Continuum theory for Higgs transition from <math>SU(2)</math> to <math>\mathbb{Z}_2</math></b>	<b>6</b>
2.1 $SU(2)$ $\pi$ -flux state	6
2.2 From $\pi$ -flux to U800	8
2.3 From $\pi$ -flux to Z3000	9
2.4 Majorana-Higgs Lagrangian	10
2.5 Symmetry-allowed couplings	11
2.5.1 Square lattice symmetries	12
2.5.2 Shastry-Sutherland symmetries	12
2.5.3 $SU(2)$ $\pi$ -flux state	13
2.5.4 U800 staggered flux state	13
2.5.5 Z3000 state	14
<b>3 Renormalization study of the critical <math>SU(2)</math> gauge theory</b>	<b>14</b>
3.1 Fermion self-energy	17
3.2 Boson self-energy	17
3.3 Renormalization of the $SO(5)$ order parameter	18
3.4 Correlation length exponent	19
3.5 Renormalization of the Yukawa coupling	21
<b>4 Conclusion and Discussion</b>	<b>23</b>
<b>A Projective symmetry group</b>	<b>25</b>
A.1 $SU(2)$ $\pi$ -flux	25
A.2 U800	25
A.3 Z3000	27
<b>B Perturbations due to pairing terms</b>	<b>27</b>
<b>C Saddle point expansion</b>	<b>28</b>
<b>D Useful integrals</b>	<b>28</b>
D.1 Fermion self-energy	29
D.2 Boson self-energy	30
D.3 $SO(5)$ vertex corrections	31
<b>References</b>	<b>32</b>

---

Quantum phase transitions in two-dimensional antiferromagnets can fall outside the conventional Landau–Ginzburg–Wilson paradigm when the critical degrees of freedom are fractionalized and coupled to emergent gauge fields. A prominent example is deconfined criticality, where continuous transitions can occur between phases with distinct broken symmetries, such as Néel order and valence-bond-solid (VBS) order [1–3]. Considerable insight into such transitions has been obtained by formulating effective field theories of Dirac fermions coupled to gauge fields; this framework provides a unified description of magnetically ordered phases, spin liquids, and their proximate critical points [4–6].

Within this fermionic framework,  $SU(2)$  gauge theories of Dirac spinons play a central role [7]. In these theories, adjoint Higgs fields reduce the gauge symmetry to  $U(1)$  or  $\mathbb{Z}_2$ , yielding staggered-flux [5] and gapless  $\mathbb{Z}_2$  Dirac spin-liquid phases [8–10], respectively. On the square lattice, such Higgs theories [11, 12] have been shown to capture deconfined critical points separating Néel order, VBS order, and gapless spin liquids, with the structure of the

low-energy theory strongly constrained by lattice symmetries and their projective symmetry group (PSG) realizations [13–15].

The Shastry–Sutherland lattice provides a natural setting in which to examine these ideas beyond the square lattice. While retaining nontrivial point-group symmetries, it breaks several lattice symmetries of the square lattice and supports additional frustration through diagonal couplings [16]. Recently, numerical [17–21] and variational studies [22] by some of us have provided evidence for a gapless  $\mathbb{Z}_2$  Dirac spin liquid stabilized in the spin-1/2 Heisenberg model on this lattice, denoted Z3000; it can be interpreted as a descendant of a staggered-flux U(1) state [5] and, ultimately, of a SU(2)  $\pi$ -flux parent state originally proposed by Affleck and Marston for square-lattice antiferromagnets [7, 8, 23–25].

A central issue in extending fermionic deconfined criticality to the Shastry–Sutherland lattice is the role of reduced lattice symmetry. Whereas it might help to microscopically stabilize quantum paramagnets from the viewpoint of ground state energy density through enhanced tuning of frustration, it also enormously broadens the scope of symmetry-allowed ground state candidates: implementing the relevant PSG requires an enlarged  $2 \times 2$  unit cell, which reorganizes the Dirac fermions and their symmetry transformations. While the square-lattice  $\pi$ -flux theory features Dirac valleys protected at distinct momenta, this protection is lifted in the Shastry–Sutherland embedding once lattice-specific perturbations are included. Furthermore, the reduced space-group symmetry enlarges the set of symmetry-allowed Yukawa couplings between fermion bilinears and Higgs fields, raising the question of whether the resulting continuum theory retains the same structure as in the square-lattice case. We show that while the reduced symmetry of the Shastry–Sutherland lattice allows for additional symmetry-allowed Yukawa couplings between Dirac fermions and Higgs fields, all such couplings share the same scaling dimension at leading order in a controlled large- $N$  expansion. Consequently, within this framework, lattice frustration does not modify the stability properties of the SO(5) critical point relative to the square-lattice theory.

The main results of this work are as follows. We construct a fermionic-spinon field theory for the Shastry–Sutherland model starting from the SU(2)  $\pi$ -flux parent state and derive the continuum perturbations that generate the U(1) staggered-flux and  $\mathbb{Z}_2$  Dirac spin-liquid descendants. The resulting continuum description is a Dirac theory coupled to an SU(2) gauge field and three real adjoint Higgs fields, whose condensates encode the Higgs transitions between these phases. At the level of the most relevant couplings controlling the Higgs transitions, the resulting Majorana–Higgs theory coincides with the corresponding square-lattice theory, including a global SO(5) symmetry [15, 26]. The reduced symmetry of the Shastry–Sutherland lattice permits additional fermion bilinears and gradient terms, but these do not change the scaling dimensions or appear only as symmetry-allowed subleading perturbations. We further determine the most general Higgs potential consistent with the microscopic symmetries and show that its structure is identical to the square-lattice case to all orders, implying the same mean-field Higgs phase structure underlying the sequence Néel  $\rightarrow \mathbb{Z}_2$  Dirac spin liquid  $\rightarrow$  VBS. Finally, we extract consequences for the competing Néel and VBS channels, including characteristic low-energy corrections to their susceptibilities.

In previous analyses for the square lattice [27, 28], it was assumed that the SO(5) breaking perturbations were strongly relevant, and this led to consideration of a critical theory without SO(5), or even Lorentz, symmetry. The present paper will take a complementary point of view, assuming that the SO(5) breaking perturbations are at best weakly relevant. We will focus on a theory with exact SO(5) symmetry, a SU(2) gauge field,  $N_f = 2$  massless, fundamental Dirac fermions and  $N_b = 2$  adjoint Higgs fields. Studies of the Néel–VBS transition on the square lattice are described by  $N_f = 2, N_b = 0$ : state-of-the-art Monte Carlo studies increasingly indicate that this SO(5) point is pseudocritical or multifractal rather than truly conformal [29–35], suggesting a wide pre-asymptotic regime with approximate SO(5) symmetry [32, 36]. These

results strongly imply the existence of a conformal fixed point with exact  $\text{SO}(5)$  symmetry for the  $N_f = 2, N_b = 2$  case, as the additional critical Higgs fields can only enhance the stability of the CFT. We will study this CFT in the large  $N_{f,b}$  expansion, and compute scaling dimensions of various observables.

Turning to the onset of the gapless  $\mathbb{Z}_2$  Dirac spin liquid, we consider the perturbative influence of the Yukawa couplings which break both  $\text{SO}(5)$  and Lorentz symmetry present for this case (for both the square and Shastry–Sutherland lattices) at the fixed point with exact  $\text{SO}(5)$  symmetry. While our renormalization-group analysis of the associated gauge theory finds the leading  $\text{SO}(5)$ -breaking perturbation to be weakly relevant at large- $N$ , and hence to destabilize the  $\text{SO}(5)$ -symmetric fixed point at the lowest energies, this does not contradict either earlier field-theoretic expectations or recent numerical work. First, the large- $N$  expansion does not control the fixed point at physical, finite  $N$  in strongly coupled gauge theories, but rather correctly identifies the operator content [37]. Second, a defining and quantitatively testable signature of such fermionic deconfined critical points is the appearance of unusually large anomalous dimensions for the competing Néel and VBS order parameters. These have been observed numerically in  $J$ – $Q$  models and related systems, and sharply distinguish deconfined criticality from conventional  $\text{O}(3)$  universality classes. In this work, we compute these anomalous dimensions analytically for the  $\text{SU}(2)$   $\pi$ -flux theory relevant to both square and Shastry–Sutherland lattices. Taken together, these results suggest that while the gapless Dirac spinon theory on the Shastry–Sutherland lattice is ultimately unstable at the lowest energies, it can remain a valid and predictive description over an extended low-energy window, which may be relevant for experimentally accessible regimes.

The remainder of the paper is organized as follows. In Sec. 1 we introduce the fermionic spinon formulation and the Z3000  $\mathbb{Z}_2$  Dirac spin-liquid *ansatz* on the Shastry–Sutherland lattice. Section 2 derives the continuum  $\text{SU}(2)$   $\pi$ -flux theory and the Higgs perturbations leading to the U800 and Z3000 states, and presents the resulting Majorana–Higgs Lagrangian and Higgs potential, together with a classification of all symmetry-allowed fermion bilinears up to gradient-order under the Shastry–Sutherland space group. Section 3 presents a renormalization-group analysis of the resulting gauge theory including a calculation of the critical exponent, and Sec. 4 discusses the implications for deconfined criticality in frustrated quantum magnets.

## 1 Gapless $\mathbb{Z}_2$ spin liquid on the Shastry–Sutherland lattice

The Shastry–Sutherland Hamiltonian for a spin-1/2 Heisenberg antiferromagnet is defined on the lattice, see Fig. 1, as

$$\hat{H} = J_s \sum_{\langle i,j \rangle_{\text{square}}} \hat{\mathbf{S}}_i \cdot \hat{\mathbf{S}}_j + J_d \sum_{\langle i,j \rangle_{\text{dimer}}} \hat{\mathbf{S}}_i \cdot \hat{\mathbf{S}}_j. \quad (1)$$

where  $\hat{\mathbf{S}}_i$  denotes the spin operator at site  $i$ , with  $J_s$  and  $J_d$  being the exchange coupling between sites  $i$  and  $j$  connecting sites along the side of the squares and dimer couplings, respectively (see Fig. 1(b)). Equation (1) accurately models the spin- $\frac{1}{2}$  Shastry–Sutherland compound  $\text{SrCu}_2(\text{BO}_3)_2$ , which realizes an exact dimer-singlet ground state at ambient pressure [38]. Hydrostatic pressure tunes the effective ratio  $J_d/J_s$ , driving a sequence of quantum phase transitions resolved by thermodynamic, spectroscopic, and neutron-scattering experiments, including an intermediate gapped plaquette phase followed by antiferromagnetic order [39, 40]. In the fermionic gauge-theory framework, increasing  $J_d/J_s$  corresponds to Higgs-induced reductions of the emergent  $\text{SU}(2)$  gauge structure, whose confined descendants naturally account for plaquette and Néel phases, providing a materials setting for pressure-driven

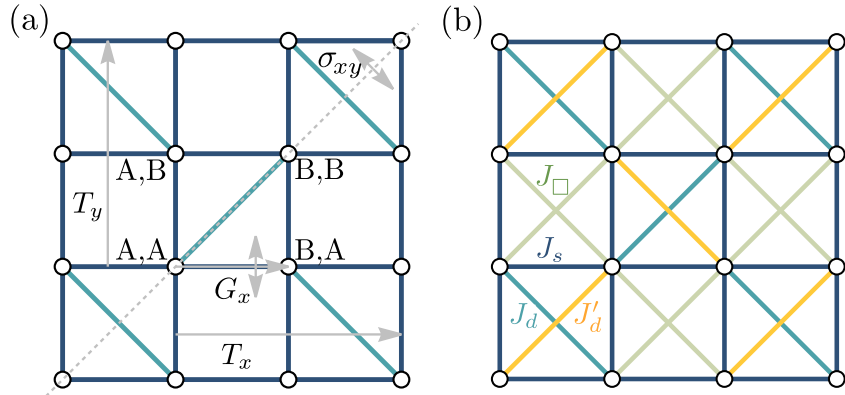


Figure 1: (a) Illustration of the Shastry–Sutherland lattice. The four orbitals within the unit cell are denoted by two sublattice degrees of freedom  $(m_x, m_y) = (A, A), (B, A), (B, B), (A, B)$ , respectively. (b) Shown are additional diagonal links with the Heisenberg couplings needed to interpolate to the square lattice limit.

deconfined or pseudocritical behavior [41, 42].

Therefore, we want to formulate the fermionic spinon theory for  $\mathbb{Z}_2$  spin liquids [43] on the Shastry–Sutherland lattice. We begin by reexpressing the spin operators with respect to spinons  $f_{i\alpha}, \alpha = \uparrow, \downarrow$  for sites  $\mathbf{i} = (i_x, i_y)$  [44]:

$$\mathbf{S}_i = \frac{1}{2} f_{i\alpha}^\dagger \boldsymbol{\sigma}_{\alpha\beta} f_{i\beta}. \quad (2)$$

Following Wen [8], we introduce a Nambu spinor

$$\psi_i = \begin{pmatrix} f_{i\uparrow} \\ f_{i\downarrow}^\dagger \end{pmatrix}, \quad (3)$$

which leads to the Bogoliubov Hamiltonian

$$H = - \sum_{ij} \psi_i^\dagger u_{ij} \psi_j. \quad (4)$$

Here,

$$u_{ij} = i u_{ij}^0 \sigma^0 + u_{ij}^a \sigma^a, \quad (5)$$

with the Pauli matrices  $\sigma^\mu$  acting on the Nambu spinor  $\psi_i$ . Spin-rotation symmetry implies that  $u_{ij}^\mu \in \mathbb{R}$  and

$$u_{ji}^0 = -u_{ij}^0, \quad u_{ji}^a = u_{ij}^a. \quad (6)$$

The spinon representation is invariant under  $SU(2)_g$  gauge transformations [7, 24] for a symmetry operator  $g$ :

$$\begin{aligned} SU(2)_g : \psi_i &\rightarrow U_{g,g(i)} \psi_{g(i)}, \\ u_{ij} &\rightarrow U_{g,g(i)} u_{g(i),g(j)} U_{g,g(j)}^\dagger. \end{aligned} \quad (7)$$

Based on a recent variational study [22] by some of us and others, a relevant candidate for the spin-liquid phase of the Shastry–Sutherland model is the stable  $\mathbb{Z}_2$  Dirac spin liquid Z3000, which can be understood as a descendant of the U800 staggered flux state, which derives from the  $SU(2)$   $\pi$ -flux state of the square lattice [8]. As the  $\mathbb{Z}_2$  *ansatz* breaks the

square lattice symmetries down to the Shastry–Sutherland lattice, we introduce 2 sublattice degrees of freedom  $m_x, m_y = A, B$  labeling the positions in the  $2 \times 2$  unit cell as shown in Fig. 1. We denote the Pauli matrices acting on  $m_x$  as  $\rho^\mu$ , and the ones acting on  $m_y$  as  $\kappa^\mu$ . In the following, when writing  $i$  or  $j$ , we reference the lattice site, whilst when writing  $r$ , we reference a  $2 \times 2$  unit cell.

Explicitly, the *ansatz* labeled by Z3000 has the following structure:

$$u_{r,A,A,r,B,A} = \begin{bmatrix} -te^{-i\theta} & 0 \\ 0 & te^{i\theta} \end{bmatrix} = u_s \quad (8)$$

$$u_{r,A,A,r,A,B} = \begin{bmatrix} te^{i\theta} & 0 \\ 0 & -te^{-i\theta} \end{bmatrix} = -u_s^\dagger \quad (9)$$

$$u_{r,A,B,r,B,B} = u_{r,B,B,r,B,A} = u_{r,B,A,r+\hat{x},A,A} = -u_s^\dagger \quad (10)$$

$$u_{r,A,B,r+\hat{y},A,A} = u_{r+\hat{y},B,A,r,B,B} = u_{r,B,B,r+\hat{x},A,B} = u_s \quad (11)$$

$$u_{r,A,A,r,B,B} = \Delta_d \sigma^x, u_{r+\hat{x},A,B,r+\hat{y},B,A} = \Delta_d \sigma^y \quad (12)$$

$$u_{r,B,B,r+\hat{x}+\hat{y},A,A} = \Delta_{d'} \sigma^x, u_{r,B,A,r,A,B} = \Delta_{d'} \sigma^y \quad (13)$$

$$u_{r,B,A,r+\hat{x},A,B} = -\Delta_{g,2} \sigma^x + \Delta_{g,1} \sigma^y \quad (14)$$

$$u_{r,A,B,r+\hat{y},B,A} = \Delta_{g,2} \sigma^x + \Delta_{g,1} \sigma^y \quad (15)$$

$$u_{r+\hat{x},A,A,r,B,B} = \Delta_{g,1} \sigma^x + \Delta_{g,2} \sigma^y \quad (16)$$

$$u_{r,B,B,r+\hat{y},A,A} = \Delta_{g,1} \sigma^x - \Delta_{g,2} \sigma^y \quad (17)$$

Equations (8)–(11) describe the fermionic hopping terms, while the remaining equations correspond to pairing terms. Depending on the parameters, this *ansatz* yields a  $\mathbb{Z}_2$  spin liquid or its parent U(1) and SU(2) states:

- i. Setting the pairing terms to zero ( $\Delta = 0$ ) and fixing  $\theta = \pi/2$  yields the parent  $\pi$ -flux state with SU(2) gauge structure. This state is labeled SU2Bn0 in Ref. [8].
- ii. Vanishing pairing ( $\Delta = 0$ ) with generic  $\theta$  leads to a U(1) state with a staggered  $(\varphi, -\varphi)$  flux through the square plaquettes, where  $\varphi = \pi + 4\theta$ . This state corresponds to U800 in Ref. [22].
- iii. Introducing finite pairing terms ( $\Delta \neq 0$ ) breaks the U(1) gauge symmetry of the U800 state down to  $\mathbb{Z}_2$ , resulting in the  $\mathbb{Z}_2$  Dirac spin liquid labeled Z3000 [22].

These hopping and pairing mean-field parameters are illustrated in Fig. 9, where the real and imaginary components of the hopping are defined as  $t_{s,0} = t \sin \theta$  and  $t_{s,z} = t \cos \theta$ , respectively.

## 2 Continuum theory for Higgs transition from SU(2) to $\mathbb{Z}_2$

### 2.1 SU(2) $\pi$ -flux state

We begin by working out the SU(2) gauge theory based on the PSG *ansatz* for the  $\pi$ -flux state [7, 8]. We replace the Nambu spinor by a matrix operator of Majorana fermions

$$\mathcal{F}_i = \begin{pmatrix} f_{i\uparrow} & -f_{i\downarrow} \\ f_{i\downarrow}^\dagger & f_{i\uparrow}^\dagger \end{pmatrix}. \quad (18)$$

This matrix operator satisfies the reality condition

$$\mathcal{F}_i^\dagger = \sigma^y \mathcal{F}_i^T \sigma^y. \quad (19)$$

$SU(2)_g$  gauge transformations  $U_g$  correspond to left multiplication

$$\mathcal{F}_i \rightarrow U_{g,g(i)} \mathcal{F}_{g(i)}, \quad (20)$$

whilst  $SU(2)$  spin rotations  $\Omega$  correspond to the right multiplication

$$\mathcal{F}_i \rightarrow \mathcal{F}_i \sigma^z \Omega_i^T \sigma^z. \quad (21)$$

The Hamiltonian Eq. (4) then reads

$$H = \sum_{\langle ij \rangle} i \alpha_{ij} \text{Tr}[\mathcal{F}_i^\dagger \mathcal{F}_j] + \beta_{ij}^a \text{Tr}[\sigma^a \mathcal{F}_i^\dagger \mathcal{F}_j] + i \gamma_{ij} \text{Tr}[\sigma^a \mathcal{F}_i^\dagger \sigma^a \mathcal{F}_j] \quad (22)$$

with

$$u_{ij} = i \alpha_{ij} \sigma^0 + \beta_{ij}^a \sigma^a. \quad (23)$$

The additional  $\gamma_{ij}$  hoppings involve projective realizations of the spin rotation symmetry [45] and will not be relevant in the following.

The  $\pi$ -flux state has hoppings  $\beta^a = 0$  and

$$\alpha_{ij} = -\alpha_{ji}, \quad \alpha_{i,i+\hat{x}} = t, \quad \alpha_{i,i+\hat{y}} = (-1)^{i_x} t. \quad (24)$$

This *ansatz* respects the square lattice symmetries and is, up to a gauge transformation, identical to the *ansatz* studied in Ref. [27]. To study the low-energy physics, we express the Hamiltonian in momentum space

$$H = -2t \sum_k \text{Tr}[\mathcal{F}_k^\dagger (\sin(k_x/2) \rho^x + \sin(k_y/2) \rho^z \kappa^x) \mathcal{F}_k], \quad (25)$$

where the summation over  $m_x, m_y$  is implicit. The Hamiltonian features a Dirac point at  $\Gamma = (0, 0)$  with a four-fold degeneracy arising from the sublattice degrees of freedom. The dispersion of the U800 spin liquid is shown in Fig. 10, where  $\phi = \pi$  corresponds to the  $SU(2)$   $\pi$ -flux state.

In comparison, on the square lattice, introducing the sublattice degree of freedom  $m_x$  is sufficient to restore translational invariance of the *ansatz*. This yields two Dirac points associated with a valley degree of freedom  $v = 0, 1$  at  $k_x = 0$  and  $k_y = 0, \pi$ . These points are back-folded to the  $\Gamma$  point due to the doubling of the unit cell in the  $y$ -direction. To make the valley degree of freedom explicit, we introduce two low-energy, two-component fermions  $\mathcal{X}_{\mathbf{r}, m_x, v}$ :

$$\mathcal{F}_{\mathbf{r}, m_x, m_y} = \sum_{m'_x} \rho_{m_x, m'_x}^x \mathcal{X}_{\mathbf{r}, m'_x, 0} + \kappa_{m_y, m_y}^z \mathcal{X}_{\mathbf{r}, m_x, 1}. \quad (26)$$

We introduce the Pauli matrices  $\mu^a$  acting on the valley degree of freedom. In the square lattice model—and by extension, the  $SU(2)$   $\pi$ -flux state of the Shastry–Sutherland model—the valleys reside at distinct momenta, which forbids intervalley scattering. However, this protection is eventually lifted by perturbations due to backfolding effects in the SS model. After explicitly verifying that there are no cross terms between  $v = 0$  and  $1$ , we find the Hamiltonian to leading order:

$$H \approx it \sum_v \text{Tr}[\mathcal{X}_v^\dagger (\rho^x \partial_x - \rho^z \partial_y) \mathcal{X}_v]. \quad (27)$$

Finally, we obtain a relativistic Dirac equation as the continuum Lagrangian

$$\mathcal{L}_{\text{MF}} = i \text{Tr}[\bar{\mathcal{X}} \gamma^\mu \partial_\mu \mathcal{X}], \quad (28)$$

where we absorbed  $t$  into the speed of light and used the Lorentz signature  $(+, -, -)$  with  $\bar{\mathcal{X}} = \mathcal{X}^\dagger \gamma^0$  and the gamma matrices  $\gamma^0 = \rho^y, \gamma^x = i\rho^z, \gamma^y = i\rho^x$ .

This theory has an emergent global symmetry  $\text{SU}(2) \times \text{SU}(2)$  given by both spin ( $\sigma$ ) and valley ( $\mu$ ) rotations [15, 27]. Imposing the reality condition Eq. (19) reduces the  $\text{SU}(2) \times \text{SU}(2)$  symmetry to  $\text{Sp}(4)$ . Since  $\text{Sp}(4)$  and  $\text{SU}(2)_g$  share the element  $-1$ , the global symmetry is given by  $\text{Sp}(4)/\mathbb{Z}_2 \cong \text{SO}(5)$ . The group action is defined by

$$\mathcal{X} \rightarrow \mathcal{X}L, \quad (29)$$

for which the reality condition implies

$$L^T = \sigma^y L^\dagger \sigma^y. \quad (30)$$

For the Lie generators  $M = M^\dagger, L = e^{iM}$ , this is equivalent to

$$M^T = -\sigma^y M \sigma^y. \quad (31)$$

The generators of  $\text{SU}(2) \times \text{SU}(2)$  that satisfy the reality condition are given by

$$T^j = \{\mu^y, \sigma^a, \mu^x \sigma^a, \mu^z \sigma^a\}, \quad (32)$$

whilst the remaining 5  $\text{SU}(4)$  generators all anti-commute and are given by

$$\Gamma^j = \{\mu^x, \mu^z, \mu^y \sigma^a\}. \quad (33)$$

They transform as a vector under the  $\text{SO}(5)$  symmetry. The corresponding fermion bilinear  $i \text{Tr}[\bar{\mathcal{X}} \Gamma^j \mathcal{X}]$  combines the VBS and Néel order parameter [13, 30, 46].

In the following subsections, we derive the continuum Lagrangian for the perturbations in Eqs. (11)–(17), which reduce the  $\pi$ -flux state to the U800 staggered-flux or Z3000 spin-liquid phases. We perform a gradient expansion of these perturbations using the low-energy modes defined in Eq. (26). By coupling these terms to adjoint Higgs fields, we capture the phase transitions to the U(1) or  $\mathbb{Z}_2$  spin liquids via Higgs condensation [11].

## 2.2 From $\pi$ -flux to U800

We obtain the continuum version of the perturbations to the U8000 spin liquid by expanding around the mean field  $u_{ij}$  in powers of  $\theta = \pi/2 + \delta\theta$  corresponding to additional hopping parameters

$$\beta_{i,i+\hat{x}}^z = -\delta\theta(-1)^{i_x+i_y}, \quad \beta_{i,i+\hat{y}}^z = \delta\theta(-1)^{i_y}. \quad (34)$$

We start with the hopping in the  $x$ -direction, where we leave the sublattice indices implicit and reintroduce the trace and  $\sigma^z$  in the Lagrangian:

$$\begin{aligned} \delta H = & -\delta\theta \sum_r [\mathcal{X}_{r,0}^\dagger \rho^x + \mathcal{X}_{r,1}^\dagger \kappa^z] \rho^x \kappa^z [\rho^x \mathcal{X}_{r,0} + \kappa^z \mathcal{X}_{r,1}] \\ & + \frac{1}{2} \delta\theta \sum_r [\mathcal{X}_{r,0}^\dagger \rho^x + \mathcal{X}_{r,1}^\dagger \kappa^z] (\rho^x - i\rho^y) \kappa^z [\rho^x \mathcal{X}_{r+\hat{x},0} + \kappa^z \mathcal{X}_{r+\hat{x},1}] \\ & + \frac{1}{2} \delta\theta \sum_r [\mathcal{X}_{r,0}^\dagger \rho^x + \mathcal{X}_{r,1}^\dagger \kappa^z] (\rho^x + i\rho^y) \kappa^z [\rho^x \mathcal{X}_{r-\hat{x},0} + \kappa^z \mathcal{X}_{r-\hat{x},1}] \quad (35) \\ \approx & 2\delta\theta \int d^2r [\mathcal{X}_{r,0}^\dagger \rho^z \partial_x \mathcal{X}_{r,1} - \mathcal{X}_{r,1}^\dagger \rho^z \partial_x \mathcal{X}_{r,0}] \\ \Rightarrow \delta\mathcal{L} = & -2i\delta\theta \text{Tr}[\sigma^z \bar{\mathcal{X}} \mu^y \gamma^y \partial_x \mathcal{X}]. \end{aligned}$$

For the hopping in the  $y$ -direction,

$$\begin{aligned}
\delta H = & +\delta\theta \sum_r [\mathcal{X}_{r,0}^\dagger \rho^x + \mathcal{X}_{r,1}^\dagger \kappa^z] \kappa^x [\rho^x \mathcal{X}_{r,0} + \kappa^z \mathcal{X}_{r,1}] \\
& -\frac{1}{2}\delta\theta \sum_r [\mathcal{X}_{r,0}^\dagger \rho^x + \mathcal{X}_{r,1}^\dagger \kappa^z] (\kappa^x - i\kappa^y) [\rho^x \mathcal{X}_{r+\hat{y},0} + \kappa^z \mathcal{X}_{r+\hat{y},1}] \\
& -\frac{1}{2}\delta\theta \sum_r [\mathcal{X}_{r,0}^\dagger \rho^x + \mathcal{X}_{r,1}^\dagger \kappa^z] (\kappa^x + i\kappa^y) [\rho^x \mathcal{X}_{r-\hat{y},0} + \kappa^z \mathcal{X}_{r-\hat{y},1}] \\
& \approx 2\delta\theta \int d^2r [\mathcal{X}_{r,0}^\dagger \rho^z \partial_x \mathcal{X}_{r,1} - \mathcal{X}_{r,1}^\dagger \rho^z \partial_x \mathcal{X}_{r,0}] \\
\Rightarrow \delta\mathcal{L} = & -2i\delta\theta \text{Tr}[\sigma^z \bar{\mathcal{X}} \mu^y \gamma^x \partial_y \mathcal{X}].
\end{aligned} \tag{36}$$

In both Eq. (35) and Eq. (36) the Pauli matrix  $\sigma^z$  is acted on by the SU(2) gauge symmetry of the  $\pi$ -flux phase. Gauge invariance hence requires the existence of similar terms with  $\sigma^x$  and  $\sigma^y$ . Therefore, we express the perturbation in a gauge-independent fashion by introducing an adjoint Higgs field  $\Phi_3^a$  with SU(2) gauge index  $a$ :

$$\delta\mathcal{L} = \Phi_3^a \text{Tr}[\sigma^a \bar{\mathcal{X}} \mu^y (\gamma^y i\partial_x + \gamma^x i\partial_y) \mathcal{X}]. \tag{37}$$

The subscript “3” is chosen in accordance with [27]. The continuum version of Eq. (35) and Eq. (36) is obtained by condensing  $\langle \Phi_3^z \rangle \propto \delta\theta$ .

### 2.3 From $\pi$ -flux to Z3000

We now turn to the pairing terms  $\Delta_d, \Delta_{d'}, \Delta_{g,1/2}$  in Eqs. (12)-(17), which break the invariant gauge group down to a  $\mathbb{Z}_2$  gauge group corresponding to the gapless Z3000 spin liquid [22]. The perturbation due to  $\Delta_d$  is given by:

$$\begin{aligned}
\delta H = & \Delta_d \text{Tr} \left\{ \sum_r \sigma^x [\mathcal{X}_{r,B,0}^\dagger + \mathcal{X}_{r,A,1}^\dagger] [\mathcal{X}_{r,A,0} - \mathcal{X}_{r,B,1}] + \text{h.c.} \right. \\
& \left. + \sigma^y [\mathcal{X}_{r,B,0}^\dagger - \mathcal{X}_{r,A,1}^\dagger] [\mathcal{X}_{r-\hat{x}+\hat{y},A,0} + \mathcal{X}_{r-\hat{x}+\hat{y},B,1}] + \text{h.c.} \right\} \\
& \approx \Delta_d \int d^2r \text{Tr}\{\sigma^x (\mathcal{X}^\dagger \rho^x \mu^z \mathcal{X} + \mathcal{X}^\dagger \rho^z \mu^x \mathcal{X})\} + \text{Tr}\{\sigma^y (\mathcal{X}^\dagger \rho^x \mu^z \mathcal{X} - \mathcal{X}^\dagger \rho^z \mu^x \mathcal{X})\} \\
\Rightarrow \delta\mathcal{L} = & \Delta_d \text{Tr}[\sigma^x \bar{\mathcal{X}} (\gamma^x \mu^z - \gamma^y \mu^x) \mathcal{X}] + \Delta_d \text{Tr}[\sigma^y \bar{\mathcal{X}} (\gamma^x \mu^z + \gamma^y \mu^x) \mathcal{X}]
\end{aligned} \tag{38}$$

$\Delta_{d'}$  leads to the same term in the Lagrangian to first order and only differs from  $\Delta_d$  by a less relevant gradient term, which we will ignore in the following.

Similarly, we can deal with  $\Delta_{g,1/2}$ . As  $\Delta_{g,2}$  vanishes to lowest order, we also calculate the gradient term in  $\Delta_{g,2}$ , see Appendix B. In summary, we obtain the following Lagrangian:

$$\begin{aligned}
\delta\mathcal{L} = & (\Delta_d + \Delta_{d'} + 2\Delta_{g,1}) (\text{Tr}[\sigma^x \bar{\mathcal{X}} (\gamma^x \mu^z - \gamma^y \mu^x) \mathcal{X}] + \text{Tr}[\sigma^y \bar{\mathcal{X}} (\gamma^x \mu^z + \gamma^y \mu^x) \mathcal{X}]) \\
& + \Delta_{g,2} (\text{Tr}[\sigma^x \bar{\mathcal{X}} (-\gamma^0 \mu^y + 1) (i\partial_x + i\partial_y) \mathcal{X}] + \text{Tr}[\sigma^y \bar{\mathcal{X}} (\gamma^0 \mu^y + 1) (i\partial_y - i\partial_x) \mathcal{X}])
\end{aligned} \tag{39}$$

Again, we want to express the Lagrangian in a gauge-invariant fashion. The first two terms are identical to the square lattice case [27], for which one can introduce two Higgs fields  $\Phi_{1,2}^a$  with the couplings

$$\Phi_1^a \text{Tr}[\sigma^a \bar{\mathcal{X}} \gamma^x \mu^z \mathcal{X}] + \Phi_2^a \text{Tr}[\sigma^a \bar{\mathcal{X}} \gamma^y \mu^x \mathcal{X}]. \tag{40}$$

Additionally to these, we obtain two gradient terms due to the  $\Delta_{g,2}$  pairing, which we can also absorb into these two Higgs fields due to them having the same symmetry transformations (see Tab. 2 to Tab. 4) leading to the terms

$$\Phi_1^a \text{Tr}[\sigma^a \bar{\mathcal{X}} (\gamma^x \mu^z - \delta(\gamma^0 \mu^y i\partial_x - i\partial_y)) \mathcal{X}] \tag{41}$$

and

$$\Phi_2^a \text{Tr}[\sigma^a \bar{\mathcal{X}}(\gamma^y \mu^x + \delta(\gamma^0 \mu^y i\partial_y - i\partial_x))\mathcal{X}], \quad (42)$$

where we defined the dimensionless scale  $\delta \equiv \Delta_{g,2}/(\Delta_d + \Delta_{d'} + 2\Delta_{g,1})$ . We note in passing that also the other pairings lead to gradient terms, which we did not compute in this work, as they will not be relevant for the renormalization group study. Their effect would add coupling terms similar to  $\delta$ . The continuum version of Eq. (39) is then obtained by condensing the Higgs fields as

$$\begin{aligned} \langle \Phi_1 \rangle &\propto (\Delta_d + \Delta_{d'} + 2\Delta_{g,1})(1, 1, 0), \\ \langle \Phi_2 \rangle &\propto (\Delta_d + \Delta_{d'} + 2\Delta_{g,1})(-1, 1, 0). \end{aligned} \quad (43)$$

## 2.4 Majorana-Higgs Lagrangian

Now, we collect the perturbations to obtain the Lagrangian for the Majorana field  $\mathcal{X}$  and 3 real, adjoint Higgs fields  $\Phi_{1,2,3}^a$ . We will not explicate the SU(2) gauge fluctuations, as they can be added via minimal coupling:

$$\begin{aligned} \mathcal{L} = &i \text{Tr}[\bar{\mathcal{X}} \gamma^\mu \partial_\mu \mathcal{X}] + \Phi_1^a \text{Tr}[\sigma^a \bar{\mathcal{X}}(\gamma^x \mu^z - \delta(\gamma^0 \mu^y i\partial_x - i\partial_y))\mathcal{X}] \\ &+ \Phi_2^a \text{Tr}[\sigma^a \bar{\mathcal{X}}(\gamma^y \mu^x + \delta(\gamma^0 \mu^y i\partial_y - i\partial_x))\mathcal{X}] \\ &+ \Phi_3^a \text{Tr}[\sigma^a \bar{\mathcal{X}} \mu^y (\gamma^y i\partial_x + \gamma^x i\partial_y)\mathcal{X}] + V(\Phi). \end{aligned} \quad (44)$$

We deduce the form of the Higgs potential  $V(\Phi)$ , which arises from integrating out the high energy spinon degrees of freedom, by constructing all gauge-invariant and symmetry-allowed terms on the Shastry-Sutherland lattice up to quartic order from Tab. 1:

	$T_x$	$T_y$	$P_x$	$P_y$	$R_{\pi/2}$	$G_x$	$\mathcal{T}$	$\sigma_{xy}$
$\Phi_1^a$	—	+	—	—	$-\Phi_2^a$	+	—	$\Phi_2^a$
$\Phi_2^a$	+	—	—	—	$-\Phi_1^a$	—	—	$\Phi_1^a$
$\Phi_3^a$	—	—	+	+	—	—	+	—

Table 1: Symmetry transformations of the Higgs fields under the square and Shastry-Sutherland lattice symmetries.

$$\begin{aligned} V(\Phi) = &s(\Phi_1^a \Phi_1^a + \Phi_2^a \Phi_2^a) + \tilde{s} \Phi_3^a \Phi_3^a + w \epsilon_{abc} \Phi_1^a \Phi_2^b \Phi_3^c \\ &+ u(\Phi_1^a \Phi_1^a + \Phi_2^a \Phi_2^a)^2 + \tilde{u}(\Phi_3^a \Phi_3^a)^2 + v_1(\Phi_1^a \Phi_2^a)^2 \\ &+ v_2(\Phi_1^a \Phi_1^a)(\Phi_2^b \Phi_2^b) + v_3[(\Phi_1^a \Phi_3^a)^2 + (\Phi_2^a \Phi_3^a)^2] \\ &+ v_4(\Phi_1^a \Phi_1^a + \Phi_2^a \Phi_2^a)(\Phi_3^b \Phi_3^b), \end{aligned} \quad (45)$$

where  $\epsilon_{abc}$  is the Levi-Civita symbol. These terms are again identical to the square lattice case [27] and lead to a mean-field diagram with 3 different phases as exemplified in Fig. 2.

In the following, we prove that the symmetry-allowed terms in the Higgs potential are identical for any lattice whose symmetry group is a superset of the Shastry-Sutherland wallpaper group  $p4g$  and a subset of the square lattice wallpaper group  $p4mm$ . To this end, we demonstrate that any term allowed on the Shastry-Sutherland lattice is also symmetry-allowed on the square lattice.

Due to invariance under  $\mathcal{T}$ , any such term is invariant under  $P_x$  and  $P_y$ , and the presence of  $G_x$  implies invariance under  $T_y$  (see Tab. 1). As we can represent the remaining generators as  $T_x = P_y \circ G_x$  and  $R_{\pi/2} = P_x \circ \sigma_{xy}$ , it is also invariant under  $T_x$  and  $R_{\pi/2}$ . Therefore, any

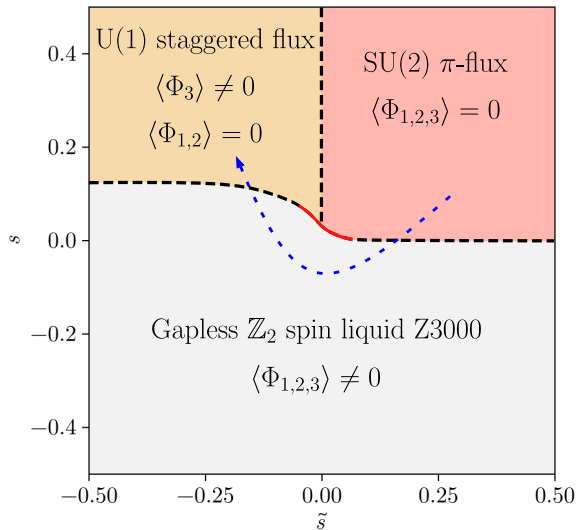


Figure 2: Mean field phase diagram of the Higgs potential in Eq. (45). The dashed (solid red) lines indicate second (first) order transitions. Following [27], we choose the mean-field parameters to be  $w = u = 1$ ,  $v_2 = -1$ ,  $\tilde{u} = 0.75$ , and  $v_4 = 0.5$ . We employ the ansatz  $\Phi_1^a = c_1 \delta_{a,x}$ ,  $\Phi_2^a = c_1 \delta_{a,y}$ , and  $\Phi_3^a = c_2 \delta_{a,z}$ . We assume that the SU(2)  $\pi$ -flux state confines to a Néel state whilst the U(1) staggered flux state confines to a columnar or plaquette VBS state. In case the confinements are opposite to our assumption, the direction of the arrow, which indicates a possible trajectory of the Shastry–Sutherland model with increasing  $J_d/J_s$ , has to be reversed. The  $\mathbb{Z}_2$  spin liquid Z3000 is a stable Dirac spin liquid [8,55]. Our field theoretic analysis shows that it is connected to Wen’s [8] gapless spin liquid Z2Azz13, consistent with an infinite density matrix renormalization group, exact diagonalization and PSG/Variational Monte Carlo study [22].

symmetry-allowed term on the Shastry–Sutherland lattice automatically satisfies square lattice symmetry, and the structure of the Higgs potential is thus identical to arbitrary order.

As has been previously argued on the square lattice [47], there exists a trivial monopole for the U(1) staggered flux state [48], which proliferates and is expected to break the U(1) spin liquid down to either Néel or VBS order [6,27]. As the Shastry–Sutherland symmetry group is a subset of the one of the square lattice, this monopole still transforms trivially under the Shastry–Sutherland symmetry group and PSG, so we expect the same instability towards Néel and VBS order.

Similarly, we expect the fate of the SU(2)  $\pi$ -flux state to lead to Néel or one of the columnar or plaquette VBS orders [30]. A large- $N_f$  analysis of the  $\pi$ -flux to  $\mathbb{Z}_2$  spin liquid transition [27] finds enhanced Néel correlations at the critical point, suggesting that the SU(2)  $\pi$ -flux state may prefer to confine to Néel order, whilst the U800 spin liquid confines to a VBS state. However, we stress that the SU(2)  $\pi$ -flux theory on its own has no preference to either phase, and that different points in the phase diagram even in the same spin liquid phase could lead to different confined phases depending on microscopic details. Therefore, it is possible that some part of the U(1) spin liquid condenses to the columnar, whilst some other condenses to the plaquette VBS order as observed numerically [3,22,49–54].

## 2.5 Symmetry-allowed couplings

In the form of Eq. (44), by ignoring the gradient terms, which have a larger scaling dimension and are thus less relevant, the critical theory is identical to the square lattice case [27]. As the

mean-field *ansatz* on the lattice might lack terms that are symmetry-allowed in the continuum theory, we now analyze all allowed fermion bilinears that respect time reversal  $\mathcal{T}$ , which acts as  $\mathcal{T} = i\sigma^y K$ , as well as lattice symmetries. For the SU(2)  $\pi$ -flux state and U800 up to nearest neighbor hopping, their PSG is consistent with the square lattice symmetries defined as

$$\begin{aligned} T_x &: (i_x, i_y) \mapsto (i_x + 1, i_y), \\ T_y &: (i_x, i_y) \mapsto (i_x, i_y + 1), \\ P_x &: (i_x, i_y) \mapsto (-i_x, i_y), \\ P_y &: (i_x, i_y) \mapsto (i_x, -i_y), \\ R_{\pi/2} &: (i_x, i_y) \mapsto (-i_y, i_x). \end{aligned} \quad (46)$$

The square lattice symmetry is explicitly broken for the Z3000 *ansatz*, which only preserves the Shastry–Sutherland symmetry group  $p4g$  as depicted in Fig. 1(a):

$$\begin{aligned} T_{2x} &: (i_x, i_y) \mapsto (i_x + 2, i_y), \\ T_{2y} &: (i_x, i_y) \mapsto (i_x, i_y + 2), \\ G_x &: (i_x, i_y) \mapsto (i_x + 1, -i_y), \\ G_y &: (i_x, i_y) \mapsto (-i_x, i_y + 1), \\ \sigma_{xy} &: (i_x, i_y) \mapsto (i_y, i_x), \\ \sigma_{x\bar{y}} &: (i_x, i_y) \mapsto (-i_y + 1, -i_x + 1), \\ C_4 &: (i_x, i_y) \mapsto (-i_y + 2, i_x - 1). \end{aligned} \quad (47)$$

The projective action for the relevant spin liquids is defined in Appendix A. For simplicity, we set all global SU(2) matrices to the identity.

### 2.5.1 Square lattice symmetries

Then, the gauge dependent Majorana fermions transform nontrivially under time reversal and the square lattice space group symmetries given by the PSG:

$$\begin{aligned} T_x &: \mathcal{X} \rightarrow \mu^x \mathcal{X}, \\ T_y &: \mathcal{X} \rightarrow \mu^z \mathcal{X}, \\ P_x &: \mathcal{X} \rightarrow -\rho^z \mu^z \mathcal{X}(-x, y), \\ P_y &: \mathcal{X} \rightarrow \rho^x \mu^x \mathcal{X}(x, -y), \\ \mathcal{T} &: \mathcal{X} \rightarrow \rho^y \mu^y \mathcal{X}, \quad i \rightarrow -i, \\ R_{\pi/2} &: \mathcal{X} \rightarrow e^{-i\pi\rho^y/4} e^{i\pi\mu^y/4} \mathcal{X}(-y, x). \end{aligned} \quad (48)$$

For the Higgs fields  $\Phi_{1,2,3}^a$ , we deduce the transformation properties in Tab. 1. By comparing with the symmetry transformations of all fermion bilinears in [15], we see that there are no other symmetry-allowed terms that one could add to the Lagrangian Eq. (44) on the square lattice.

### 2.5.2 Shastry–Sutherland symmetries

The Shastry–Sutherland lattice breaks symmetries of the square lattice. Thus, we can use the transformation properties of  $\mathcal{X}$  in Eq. (48) to derive the action of the Shastry–Sutherland point group, which can be generated by  $G_x$  and  $\sigma_{xy}$  [22]. These can be expressed with respect to the square lattice symmetry generators as

$$G_x = P_y \circ T_x, \quad \sigma_{xy} = P_x \circ R_{\pi/2}. \quad (49)$$

$T^j$	$G_x$	$\mathcal{T}$	$\sigma_{xy}$
$\mu^y$	—	—	+
$\sigma^a$	—	—	—
$\mu^x\sigma^a$	—	+	$-\mu^z\sigma^a$
$\mu^z\sigma^a$	—	+	$-\mu^x\sigma^a$

Table 2: Transformation of  $\text{Tr}[\sigma^a \bar{\mathcal{X}} T^j \mathcal{X}]$  under the Shastry–Sutherland symmetries.  $T^j = \{\mu^y, \sigma^a, \mu^x\sigma^a, \mu^z\sigma^a\}$  are the 10 generators of  $\text{SO}(5)$ .

$\Gamma^j \gamma^\mu$	$G_x$	$\mathcal{T}$	$\sigma_{xy}$
$\mu^x\gamma^0$	+	+	$\mu^z\gamma^0$
$\mu^x\gamma^x$	+	—	$\mu^z\gamma^y$
$\mu^x\gamma^y$	—	—	$\mu^z\gamma^x$
$\mu^z\gamma^0$	+	+	$\mu^x\gamma^0$
$\mu^z\gamma^x$	+	—	$\mu^x\gamma^y$
$\mu^z\gamma^y$	—	—	$\mu^x\gamma^x$
$\mu^y\sigma^a\gamma^0$	+	+	—
$\mu^y\sigma^a\gamma^x$	+	—	$-\mu^y\sigma^a\gamma^y$
$\mu^y\sigma^a\gamma^y$	—	—	$-\mu^y\sigma^a\gamma^x$

Table 3: Transformation of  $\text{Tr}[\sigma^a \bar{\mathcal{X}} \Gamma^j \gamma^\mu \mathcal{X}]$  under the Shastry–Sutherland symmetries.  $\Gamma^j = \{\mu^x, \mu^z, \mu^y\sigma^a\}$  transforms as a vector under  $\text{SO}(5)$ .

On the low-energy degrees of freedom, they act as

$$\begin{aligned} G_x : \mathcal{X} &\rightarrow \rho^x \mathcal{X}(x, -y), \\ \mathcal{T} : \mathcal{X} &\rightarrow \rho^y \mu^y \mathcal{X}, \quad i \rightarrow -i, \\ \sigma_{xy} : \mathcal{X} &\rightarrow -\rho^z \mu^z e^{-i\pi\rho^y/4} e^{i\pi\mu^y/4} \mathcal{X}(y, x). \end{aligned} \quad (50)$$

We tabulated all possible bilinears up to first-order gradient terms in Tab. 2 to Tab. 4. We color code all fermion bilinears, which do not transform under spin and are consistent with the transformation properties of the Higgs fields in Tab. 1. For  $\Phi_3$ , there are only additional gradient terms, whilst for  $\Phi_{1/2}$ , we have additional zeroth-order bilinears and gradient terms. As the gradient terms are less relevant, we can ignore them. The zeroth-order bilinears change the coupling between the Higgs fields and Dirac fermions but as we will show in Sec. 3, this does not alter the scaling dimensions of the quantum field theory.

### 2.5.3 $\text{SU}(2)$ $\pi$ -flux state

This phase corresponds to no Higgs condensate  $\langle \Phi_{1,2,3}^a \rangle = 0$  and possesses an  $\text{SU}(2)$  gauge symmetry as well as an emergent  $\text{SO}(5)$  symmetry as discussed in Sec. 2.1. The theory is believed to confine to the Néel or VBS phase [30, 31].

### 2.5.4 U800 staggered flux state

The staggered flux state corresponds to condensing  $\langle \Phi_3^a \rangle \propto \delta\theta\delta_{a,z}$ . This theory has a single gauge boson, which we believe as discussed in Sec. 2.4 and [27] likely confines to a VBS state,

$\mu^y \gamma^\mu i\partial_\nu$	$G_x$	$\mathcal{T}$	$\sigma_{xy}$	$\mu^{0,x,y} i\partial_\mu$	$G_x$	$\mathcal{T}$	$\sigma_{xy}$
$\mu^y \gamma^0 i\partial_0$	+	+	-	$i\partial_0$	-	+	-
$\mu^y \gamma^0 i\partial_x$	+	-	$-\mu^y \gamma^0 i\partial_y$	$i\partial_x$	-	-	$-i\partial_y$
$\mu^y \gamma^0 i\partial_y$	-	-	$-\mu^y \gamma^0 i\partial_x$	$i\partial_y$	+	-	$-i\partial_x$
$\mu^y \gamma^x i\partial_0$	+	-	$-\mu^y \gamma^y i\partial_0$	$\mu^x i\partial_0$	-	-	$-\mu^z i\partial_0$
$\mu^y \gamma^x i\partial_x$	+	+	$-\mu^y \gamma^y i\partial_y$	$\mu^x i\partial_x$	-	+	$-\mu^z i\partial_y$
$\mu^y \gamma^x i\partial_y$	-	+	$-\mu^y \gamma^y i\partial_x$	$\mu^x i\partial_y$	+	+	$-\mu^z i\partial_x$
$\mu^y \gamma^y i\partial_0$	-	-	$-\mu^y \gamma^x i\partial_0$	$\mu^z i\partial_0$	-	-	$-\mu^x i\partial_0$
$\mu^y \gamma^y i\partial_x$	-	+	$-\mu^y \gamma^x i\partial_y$	$\mu^z i\partial_x$	-	+	$-\mu^x i\partial_y$
$\mu^y \gamma^y i\partial_y$	+	+	$-\mu^y \gamma^x i\partial_x$	$\mu^z i\partial_y$	+	+	$-\mu^x i\partial_x$

Table 4: Transformation of  $\text{Tr}[\sigma^a \bar{\mathcal{X}} i\partial_\mu \mathcal{X}]$ ,  $\text{Tr}[\sigma^a \bar{\mathcal{X}} \Gamma^j i\partial_\mu \mathcal{X}]$ , and  $\text{Tr}[\sigma^a \bar{\mathcal{X}} T^j \gamma^\mu i\partial_\nu \mathcal{X}]$  under the Shastry–Sutherland symmetries. We only consider terms that do *not* transform under spin [15].

but possibly also the Néel phase [6, 48].

### 2.5.5 Z3000 state

The Z3000 state corresponds to condensing  $\langle \Phi_{1,2}^a \rangle \neq 0$ . Due to the symmetry transformations between the two fields, there is only a single tuning parameter  $s$  to condense them and the existence of the term  $w$  implies that also  $\langle \Phi_3^a \rangle \propto w \epsilon_{abc} \langle \Phi_1^b \rangle \langle \Phi_2^c \rangle$  condenses.

As was shown in a recent PSG study [22], this spin liquid is related to the Z2Azz13 spin liquid on the square lattice [8]. This is consistent with our conclusion that up to less relevant gradient terms the continuum theory is identical to the one on the square lattice [27]. Similarly, the structure of the symmetry-allowed Higgs potential is identical for the two systems to arbitrary order in the Higgs fields.

## 3 Renormalization study of the critical SU(2) gauge theory

The stability of the emergent  $\text{SO}(5)$  symmetry at the deconfined quantum critical point remains a subject of active debate. While the fermionic  $\text{SU}(2)$   $\pi$ -flux theory exhibits an enlarged  $\text{SO}(5)$  symmetry that unifies the Néel and valence-bond-solid order parameters [1, 2, 29, 30], a growing body of analytical and numerical work indicates that this fixed point is generically unstable in the strict infrared due to symmetry-allowed perturbations, most notably the Yukawa coupling between Dirac spinons and Higgs fields [30, 31, 56]. Importantly, this instability does not preclude the appearance of robust  $\text{SO}(5)$ -symmetric scaling over extended intermediate length scales. Instead, it is now widely understood that the  $\text{SO}(5)$  fixed point acts as a pseudocritical or “walking” fixed point, controlling a broad pre-asymptotic regime before renormalization-group flows ultimately run away at the lowest energies [32, 35, 36, 57]. This picture reconciles large- $N$  field-theoretic analyses with state-of-the-art Monte Carlo simulations, which consistently observe approximate  $\text{SO}(5)$  symmetry, emergent operator degeneracies, and universal scaling over many decades despite an eventual departure from true conformality. In this sense, the  $\text{SO}(5)$  theory provides the appropriate organizing framework for both the square-lattice and Shastry–Sutherland antiferromagnets, even though it does not represent a stable infrared fixed point. To assess the ultimate fate of this fixed point, we reformulate the theory in terms

of  $N_f = 2$  flavors of complex Dirac fermions, generalizing the model to include  $v = 1, \dots, N_f$  valleys and a Higgs flavor index  $\alpha = 1, \dots, N_b/2$  to facilitate a controlled expansion.

The Dirac fermions can be expressed with respect to the Majorana matrix operator as

$$\psi_{a,m_x,v} = i\sigma_{ab}^y [\mathcal{X}_{m_x,v}]_{1,b}. \quad (51)$$

Introducing the SU(2) gauge field  $A_\mu^a$  via minimal coupling leads to the effective Lagrangian:

$$\begin{aligned} \mathcal{L} &= \mathcal{L}_\psi + \mathcal{L}_\Phi + \mathcal{L}_{\Phi\psi}, \\ \mathcal{L}_\psi &= i\bar{\psi}_v \gamma^\mu (\partial_\mu - iA_\mu^a \sigma^a) \psi_v, \\ \mathcal{L}_\Phi &= \frac{1}{2g} [(\partial_x \Phi_1^a - 2\epsilon_{abc} A_x^b \Phi_1^c)^2 + (\partial_y \Phi_2^a - 2\epsilon_{abc} A_y^b \Phi_2^c)^2] + \dots, \\ \mathcal{L}_{\Phi\psi} &= y \sum_\alpha (\Phi_{1\alpha}^a \bar{\psi} \mu^z \gamma^x \sigma^a \psi + \Phi_{2\alpha}^a \bar{\psi} \mu^x \gamma^y \sigma^a \psi). \end{aligned} \quad (52)$$

This field theory is identical to the square lattice case [27, 28]. Therefore, we can conclude that also on the level of the quantum field theory the spin liquid and the associated transitions towards the Néel and VBS phase on the square lattice can be connected to the ones on the Shastry–Sutherland antiferromagnet. Unlike previous work in the  $y \rightarrow \infty$  limit [27], which breaks the emergent SO(5) symmetry and also Lorentz invariance, we will study the SO(5) critical point by considering  $y$  as a perturbation and gauging the effect of the Yukawa coupling on the stability on the phase in this perturbative expansion. We want to emphasize that the following field-theoretic analysis applies to both the square as well as the Shastry–Sutherland Heisenberg antiferromagnet.

The analysis in this section focuses on the SO(5) symmetric theory at  $y = 0$ , which is expected to be exactly conformal. The influence of a non-zero  $y$  will be addressed finally in Section 3.5.

As all symmetry-allowed terms should be present in the Lagrangian, we will add a quadratic minimally-coupled kinetic term for each boson  $\Phi_{s,\alpha}^a$ ,  $\alpha = 1, \dots, N_b/2$ ,  $s = 1, 2$ ,  $a = 1 \dots 3$  in all space-time directions. In general, these terms could have different coupling constants, but we will assume they coincide in the following. This leads to the following theory:

$$\begin{aligned} \mathcal{L}_\psi &= i\bar{\psi}_v \gamma^\mu (\partial_\mu - iA_\mu^a \sigma^a) \psi_v, \\ \mathcal{L}_\Phi &= \frac{1}{2g} [(\delta_{ac} \partial_\mu - 2\epsilon_{abc} A_\mu^b) \Phi_{sa}^c]^2, \\ \mathcal{L}_{\Phi\psi} &= y \sum_{s,\alpha} \Phi_{sa}^a \bar{\psi} X^s \sigma^a \psi, \end{aligned} \quad (53)$$

where  $X^s = (\mu^z \gamma^x, \mu^x \gamma^y)$  and  $s = 1, 2$ . To resolve the constraint  $\sum_{s,\alpha} (\Phi_{sa}^a)^2 = 1$ , we add a real valued field  $\lambda$  as a Lagrange multiplier, which allows us to write the bosonic action by rescaling  $\Phi_{sa}^a \rightarrow \sqrt{\frac{g}{3N_b}} \Phi_{sa}^a$  as

$$\mathcal{L}_\Phi = \frac{1}{2g} \left[ ((\delta_{ac} \partial_\mu - 2\epsilon_{abc} A_\mu^b) \Phi_{sa}^c)^2 + i\lambda \left( (\Phi_{sa}^a)^2 - \frac{3N_b}{g} \right) \right]. \quad (54)$$

We now follow [58] to obtain the saddle-point equation in the large  $N_b$  limit: One can first eliminate  $A_\mu$  by minimizing  $S$  with respect to  $A_\mu$ . Then, we integrate out the bosons leading to

$$S_b = \frac{3}{g} \int d^3r \left( -\frac{N_b i\lambda}{2g} - \frac{N_b}{2} \log \det | -\partial_\mu^2 + i\lambda | \right). \quad (55)$$

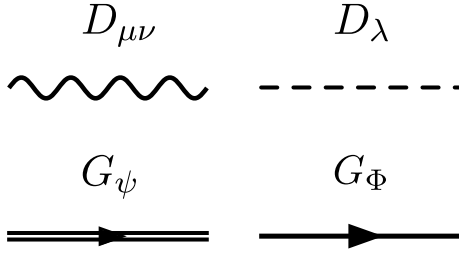


Figure 3: Definition of diagrammatic symbols for the propagators  $D_{\mu\nu}$ ,  $D_\lambda$ ,  $G_\psi$ , and  $G_\Phi$ .

For large  $N_b$ , the only relevant contributions to the path integral are at the saddle point, which we can obtain by varying the action with respect to  $\lambda$ :

$$\frac{N_b i}{2g} = -\frac{N_b}{2} \frac{\delta}{\delta \lambda} \log \det | -\partial_\mu^2 + i\lambda | = -\frac{N_b i}{2} G_\Phi(x, x), \quad (56)$$

where we have introduced the Green's function

$$G_\Phi = (-\partial_\mu^2 + i\lambda)^{-1}. \quad (57)$$

We can solve the saddle point equation by going to momentum space with  $G_\Phi^{-1} = k^2 + i\lambda$ :

$$\frac{1}{g} = \int \frac{d^3 k}{8\pi^3} \frac{1}{k^2 + i\lambda}. \quad (58)$$

This is solved by  $r = i\lambda_0$  with  $G_\Phi(k) = (k^2 + r)^{-1}$ . For large  $N_b$  this theory becomes critical when  $r = 0$  [59].

We now obtain the effective gauge theory for  $\lambda$  and  $A_\mu^a$  at  $T = 0$  by expanding around the saddle point leading to a correction to the action

$$\mathcal{F} = \frac{1}{2} \int \frac{d^3 p}{(2\pi)^3} \left( \Pi_\lambda \lambda^2 + \Pi_A \left( \delta_{\mu\nu} - \frac{p_\mu p_\nu}{p^2} \right) A_\mu^a A_\nu^a \right), \quad (59)$$

where

$$\begin{aligned} \Pi_\lambda(p, r) &= \frac{3N_b}{4\pi p} \arctan \frac{p}{2\sqrt{r}}, \\ \Pi_A(p, r) &= N_f \frac{p}{16} + 8N_b \left[ \frac{p^2 + 4r}{8\pi p} \arctan \frac{p}{2\sqrt{r}} - \frac{\sqrt{r}}{4\pi} \right]. \end{aligned} \quad (60)$$

Details are given in Appendix C. The propagators are shown in Fig. 3 and can be obtained by imposing the gauge  $k_\mu A_\mu = 1 - \zeta$ :

$$\begin{aligned} D_\lambda &= \langle \lambda \lambda \rangle = \frac{1}{\Pi_\lambda}, \\ D_{\mu\nu}^{ab} &= \langle A_\mu^a A_\nu^b \rangle = \frac{\delta_{ab}}{\Pi_A} \left( \delta_{\mu\nu} - \zeta \frac{p_\mu p_\nu}{p^2} \right), \\ G_\Phi^{ab} &= \frac{\delta_{ab}}{k^2 + r}, \\ G_\psi &= \frac{k}{k^2}. \end{aligned} \quad (61)$$

As we are interested in the critical point, we will set  $r = 0$  in the following, so the polarizations of Eq. (60) simplify to

$$\Pi_\lambda(p) = \frac{3N_b}{8p}, \quad \Pi_A(p) = (N_f + 8N_b) \frac{p}{16}. \quad (62)$$

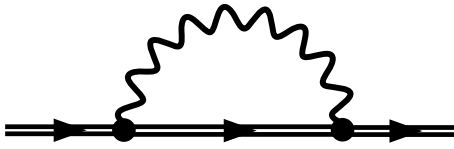


Figure 4: Self-energy correction to the fermion propagator due to the gauge field.

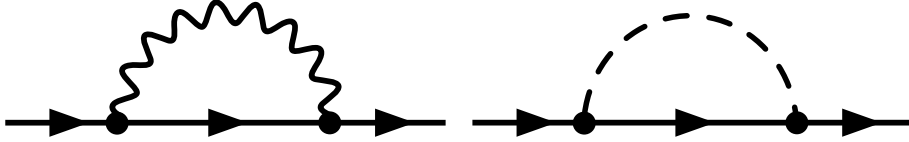


Figure 5: Self-energy corrections to the Higgs propagator due to the gauge field and the Lagrange multiplier field.

### 3.1 Fermion self-energy

The scaling dimension of  $\psi$  is defined as

$$\dim[\psi] = \frac{D - 1 + \eta_\psi}{2} \quad (63)$$

with  $D = 3$  and the anomalous dimension  $\eta_\psi$ . We can evaluate  $\eta_\psi$  by calculating the lowest order self-energy graph  $\Sigma(k)$  due to the gauge field, see Fig. 4, and picking up the logarithmically divergent  $\log k$  part:

$$\Sigma_\psi(k) = \sigma^a \sigma^a \int \frac{d^3 q}{(2\pi)^3} \gamma_\mu G_\psi(k+q) \gamma_\nu D_{\mu\nu}(-q) \rightarrow \frac{8}{(N_f + 8N_b)\pi^2} (1 - 3\zeta) \log k. \quad (64)$$

Details are given in Appendix D. This gives the gauge-dependent anomalous dimension

$$\eta_\psi = \frac{8(1 - 3\zeta)}{(N_f + 8N_b)\pi^2} \quad (65)$$

and the overall fermion scaling dimension

$$\dim[\psi] = 1 + \frac{\eta_\psi}{2} = 1 + \frac{4}{(N_f + 8N_b)\pi^2} (1 - 3\zeta). \quad (66)$$

### 3.2 Boson self-energy

The scaling dimension of the Higgs fields  $\Phi$  is similarly given by

$$\dim[\Phi] = \frac{D - 2 + \eta_\Phi}{2} \quad (67)$$

with anomalous dimension  $\eta_\Phi$ . We can obtain that to  $\mathcal{O}(1/N)$  order by extracting the  $\log k$  divergence of the contributing diagrams in Fig. 5. We begin with the corrections due to the gauge field:

$$\begin{aligned} I_{A;1} &= 8 \int \frac{d^3 q}{(2\pi)^3} G_\Phi(k+q) D_{\mu\nu}(-q) (2k+q)_\mu (2k+q)_\nu, \\ &\rightarrow -\frac{8 \cdot 4}{(N_f + 8N_b)\pi^2} \left( \frac{10}{3} + 2\zeta \right) k^2 \log k. \end{aligned} \quad (68)$$

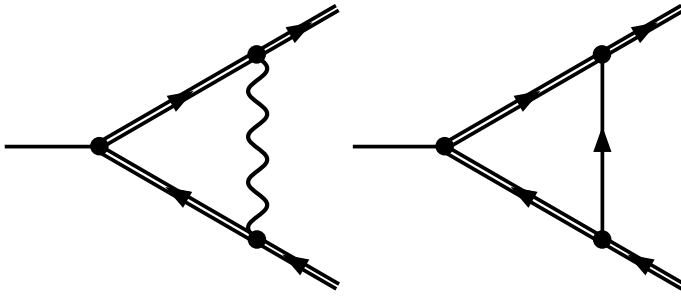


Figure 6: Vertex corrections to the SO(5) order parameter due to the gauge field and the Yukawa coupling of the fermions to the Higgs fields.

The factor of 8 is due to the gauge indices

$$2\epsilon_{abc} \cdot 2\epsilon_{fbc} = 8\delta_{af}, \quad (69)$$

where  $a$  and  $f$  are the ingoing and outgoing gauge indices of the bosons.

For the Lagrange multiplier fluctuations, we obtain

$$I_{\lambda;1} = i^2 \int \frac{d^3 q}{(2\pi)^3} G_\Phi(k+q) D_\lambda(-q) \rightarrow \frac{4}{9N_b \pi^2} k^2 \log k. \quad (70)$$

Therefore, we can conclude

$$\eta_\Phi = -\frac{32}{(N_f + 8N_b)\pi^2} \left( \frac{10}{3} + 2\zeta \right) + \frac{4}{9N_b \pi^2}. \quad (71)$$

### 3.3 Renormalization of the SO(5) order parameter

As discussed in Sec. 2.1, the  $\pi$ -flux state possesses an emergent SO(5) symmetry combining the Néel and VBS order parameters into the 5-vector

$$i \text{Tr}[\bar{\mathcal{X}} \Gamma^j \mathcal{X}] \quad (72)$$

with

$$\Gamma^j = \{\mu^x, \mu^z, \mu^y \sigma^a\}. \quad (73)$$

The first two components correspond to the VBS order, whilst the latter 3 correspond to the Néel order. We begin by expressing the VBS order parameter with respect to the Dirac fermions in Eq. (51):

$$V^i = (\bar{\psi} \mu^x \psi, \bar{\psi} \mu^z \psi). \quad (74)$$

For the Néel order, we will only consider the  $\hat{z}$ -component. The renormalization of the other components is identical due to SU(2) symmetry:

$$N^z = \bar{\psi} \mu^y \psi. \quad (75)$$

We therefore have to study the anomalous dimensions of the bilinears  $n^i = \bar{\psi} \mu^i \psi$  with  $i = x, y, z$ , which we do by introducing a source field  $J^i$  and calculating the vertex corrections as shown in Fig. 6. We begin with the corrections due to the gauge field:

$$\begin{aligned} I_{A;2} &= 3 \int \frac{d^3 q}{(2\pi)^3} \gamma_\mu G_\psi(k_1 + q) G_\psi(k_2 + q) \gamma_\nu D_{\mu\nu}(-q) \\ &\rightarrow \frac{3 \cdot 8\mu^i}{(N_f + 8N_b)\pi^2} (\zeta - 3) \log k, \end{aligned} \quad (76)$$

where we restricted ourselves to the case  $k_1 = k_2 \equiv k$ .

The corrections due to the Higgs field do not have a logarithmic divergence, so they can be ignored. We can now collect the vertex contribution as well as the self-energy correction to the fermion bilinear:

$$\dim[\bar{\psi}\mu^i\psi] = 2\dim[\psi] + \eta_{\text{vrtx}} = 2 - \frac{64}{(N_f + 8N_b)\pi^2}. \quad (77)$$

Reassuringly, this result is gauge-invariant. Compared to e.g. [59], the corrections to the scaling dimension are a factor of 3 larger due to having an SU(2) instead of U(1) gauge field. Both VBS and Néel order parameter get the same correction.

We can use this to obtain the correction to the scaling of the susceptibility

$$\chi(k) = \langle \bar{\psi}\Gamma^i\psi(k)\bar{\psi}\Gamma^j\psi(-k) \rangle \sim |k|^{1-\frac{128}{(N_f + 8N_b)\pi^2}} \sim |k|^{0.279} \quad (78)$$

for the physically relevant values  $N_f = N_b = 2$ .

The positive exponent implies that the susceptibility is suppressed as  $k \rightarrow 0$ , a signature of the large anomalous dimension  $\eta$  associated with deconfined quantum criticality [2]. In real space, the susceptibility follows the dual scaling:

$$\chi(r) \sim |r|^{-4+\frac{128}{(N_f + 8N_b)\pi^2}} \approx |r|^{-3.279}. \quad (79)$$

Equation (79) implies a large anomalous dimension  $\eta_{\text{SO}(5)} \approx 0.360$  for the SO(5) order parameter in the physical case  $N_f = N_b = 2$ . This manifests as a strong enhancement of the Néel and VBS susceptibilities at long distances, in sharp contrast to the O(3) universality class [57, 60]. Such large anomalous dimensions are a hallmark of fermionic deconfined quantum criticality and reflect the fractionalized nature of the critical degrees of freedom.

Interestingly, large anomalous dimensions of comparable magnitude have been reported in numerical studies of  $J$ - $Q$  models, which find  $\eta \approx 0.3$ – $0.35$  for the Néel–VBS order parameter [61]. While our analytical result is obtained in a controlled large- $N$  expansion and is not expected to be quantitatively precise, the close agreement in scale supports the interpretation of both systems as exhibiting pseudocritical SO(5)-symmetric behavior governed by fractionalized degrees of freedom.

### 3.4 Correlation length exponent

We compute the correlation length exponent  $\nu$  defined via

$$\xi \propto (g - g_c)^{-\nu}, \quad (80)$$

following [59]. The critical exponent is related to

$$\nu = \frac{\gamma_\Phi}{2 - \eta_\Phi}, \quad (81)$$

where  $\eta_\Phi$  is the anomalous dimension of the Higgs fields and  $\gamma_\Phi$  is defined as the scaling of the mass to 0 at the critical point:

$$G_\Phi^{-1}(k=0) \sim (g - g_c)^{\gamma_\Phi}. \quad (82)$$

Analogously to [59], we define

$$\frac{1}{g_c} - \frac{1}{g} = \frac{\sqrt{r_g}}{4\pi}. \quad (83)$$

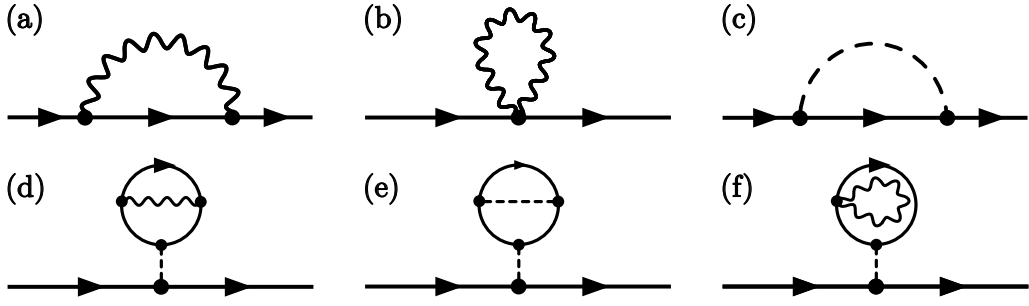


Figure 7: Self-energy diagrams of  $\Phi$  at order  $\mathcal{O}(1/N)$ . At the critical point, only (a) and (c) contribute. These diagrams are used to calculate  $\gamma_\Phi$  and via the scaling relation,  $\gamma_\Phi = \nu(2 - \eta_\Phi)$ , the correlation length exponent.

As shown in [59],  $\gamma_\Phi$  is related to the coefficient  $\alpha$  of the logarithmic divergence  $r_g \log(r_g)$  of  $\Sigma(0, r) - \frac{\Pi_\lambda(0, 0)}{\Pi_\lambda(0, r)} \Sigma(0, 0)$  via

$$\gamma_\Phi = 2(1 - \alpha). \quad (84)$$

We will thus calculate  $\alpha$  in the following. The contributing diagrams are shown in Fig. 7, and their contributions to the self-energy are:

$$\begin{aligned} \Sigma^{(a)} &= I_{A;1}, \\ \Sigma^{(b)} &= 8 \sum_{\mu, \nu} \int \frac{d^3 q}{(2\pi)^3} \frac{1}{\Pi_A(q)} \left( \delta_{\mu\nu} - \zeta \frac{q_\mu q_\nu}{q^2} \right), \\ \Sigma^{(c)} &= I_{\lambda;1}, \\ \Sigma^{(d)} &= \frac{i^2}{\Pi_\lambda(0, r)} \int \frac{d^3 q}{(2\pi)^3} 3N_b G_\Phi(q)^2 I_{A;1}(q), \\ \Sigma^{(e)} &= \frac{i^2}{\Pi_\lambda(0, r)} \int \frac{d^3 q}{(2\pi)^3} 3N_b G_\Phi(q)^2 I_{\lambda;1}(q), \\ \Sigma^{(f)} &= \frac{i^2 \Sigma^{(b)}}{\Pi_\lambda(0, r)} \int \frac{d^3 q}{(2\pi)^3} 3N_b G_\Phi(q)^2 = -\Sigma^{(b)}. \end{aligned} \quad (85)$$

For  $\Sigma = \Sigma^{(c)} + \Sigma^{(e)}$ , we get the contribution

$$\alpha_\lambda = \frac{2}{N_b \pi^2}. \quad (86)$$

We now look at the gauge contributions  $\Sigma = \Sigma^{(a)} + \Sigma^{(d)}$ : All steps in [59] up to Eq. (31) still hold true for our case with an additional factor of 8 leading to

$$\begin{aligned} \Sigma(0, r) - \frac{\Pi(0, 0)}{\Pi(0, r)} \Sigma(0, 0) &= 8 \int \frac{q^2 dq}{2\pi^2} \left[ \frac{1 - \zeta}{\Pi_A(q, r_g)} \frac{q^2}{q^2 + r_g} \right. \\ &\quad \left. - \frac{3N_b}{\Pi_\lambda(0, r_g)} \frac{I_A(q, r_g)}{\Pi_A(q, r_g)} + \frac{3N_b}{\Pi_\lambda(0, r_g)} \frac{1}{4q \Pi_A(q, 0)} \right], \end{aligned} \quad (87)$$

where  $I_a$  is defined as in [59] and evaluates to

$$I_A(q, r_g) \approx (1 - \zeta) \frac{\Pi_\lambda(0, r_g)}{3N_b} + \frac{1}{4q} - \frac{\sqrt{r_g}}{\pi q^2}. \quad (88)$$

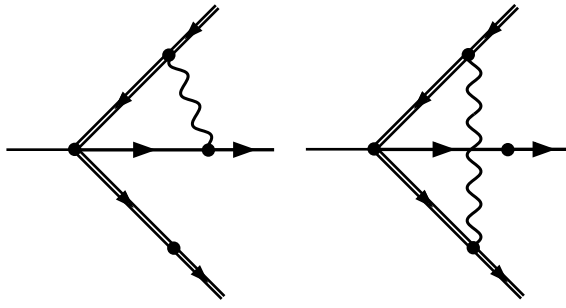


Figure 8: Vertex corrections to the Yukawa coupling. The first diagram contributes two times by coupling to the other fermion line.

By expanding up to  $1/q^3$  for large  $q$ , we obtain the logarithmic divergence

$$\alpha_A = -\frac{8 \cdot 4}{\pi^2(N_f + 8N_b)} \left( \zeta + \frac{7N_f - 8N_b}{N_f + 8N_b} \right). \quad (89)$$

Overall, we have  $\alpha = \alpha_\lambda + \alpha_A$  and

$$\gamma_\Phi = 2(1 - \alpha) = 2 - \frac{4}{N_b \pi^2} + \frac{64}{\pi^2} \left( \frac{7N_f - 8N_b}{(N_f + 8N_b)^2} + \frac{\zeta}{N_f + 8N_b} \right). \quad (90)$$

We can now calculate the correlation length exponent:

$$\begin{aligned} \nu &= \frac{\gamma_\Phi}{2 - \eta_\Phi} \approx \frac{\gamma_\Phi}{2} \left( 1 + \frac{\eta_\Phi}{2} \right) \\ &= \left[ 1 - \frac{2}{N_b \pi^2} + \frac{32}{\pi^2} \left( \frac{7N_f - 8N_b}{(N_f + 8N_b)^2} + \frac{\zeta}{N_f + 8N_b} \right) \right] \left[ 1 + \frac{2}{9N_b \pi^2} - \frac{16}{(N_f + 8N_b) \pi^2} \left( \frac{10}{3} + 2\zeta \right) \right] \\ &\approx 1 - \frac{16}{9N_b \pi^2} + \frac{32}{\pi^2} \frac{7N_f - 8N_b}{(N_f + 8N_b)^2} - \frac{160}{3(N_f + 8N_b) \pi^2}. \end{aligned} \quad (91)$$

This result is, as expected, gauge-independent. For the physically relevant  $N_f = N_b = 2$ , we get  $\nu \approx 0.590$ .

### 3.5 Renormalization of the Yukawa coupling

Finally, we want to study the stability of the SO(5) critical point by calculating the vertex corrections to the scaling dimension of the Yukawa coupling  $y$ , which breaks the SO(5) symmetry. To this end, we will couple the Yukawa terms to a source field and consider the vertex corrections due to the gauge field. The contributing diagrams are shown in Fig. 8, the first one contributes twice due to the choice of the Dirac fermion to interact with the boson. We begin with the first diagram and set all external momenta to 0, as we are only interested in the logarithmic divergence:

$$\begin{aligned} I_{\Phi\psi} &= (-i\sigma^b)\sigma^c \int \frac{d^3 q}{(2\pi)^3} \gamma_\mu G_\psi(q) X^s G_\Phi(q) q_\nu (2\epsilon_{abc}) D_{\mu\nu}(-q) \\ &= \frac{4 \cdot 16\sigma^a}{N_f + 8N_b} \int \frac{d^3 q}{(2\pi)^3} \left[ \frac{q X^s q}{q^5} - \zeta \frac{X^s}{q^3} \right] \rightarrow \frac{4 \cdot 16\sigma^a X^s}{6(N_f + 8N_b)\pi^2} (1 + 3\zeta) \log k, \end{aligned} \quad (92)$$

and the second diagram:

$$\begin{aligned}
I_{\psi\psi} &= \sigma^b \sigma^a \sigma^b \int \frac{d^3 q}{(2\pi)^3} \gamma_\mu G_\psi(q) X^s G_\psi(q) \gamma_\nu D_{\mu\nu}(-q) \\
&= -\sigma^a \frac{16}{N_f + 8N_b} \int \frac{d^3 q}{(2\pi)^3} \gamma_\mu \frac{q X^s q}{q^5} \gamma_\nu \left( \delta_{\mu\nu} - \zeta \frac{q_\mu q_\nu}{q^2} \right) \\
&= -\sigma^a \frac{16}{N_f + 8N_b} \int \frac{d^3 q}{(2\pi)^3} \left[ \frac{\gamma_\mu q X^s q \gamma_\mu}{q^5} - \zeta \frac{X^s}{q^3} \right] \\
&= \sigma^a \frac{16}{N_f + 8N_b} \int \frac{d^3 q}{(2\pi)^3} \left[ \frac{q X^s q}{q^5} + \zeta \frac{X^s}{q^3} \right] \\
&\rightarrow \sigma^a X^s \frac{16}{6(N_f + 8N_b)\pi^2} (1 - 3\zeta) \log k.
\end{aligned} \tag{93}$$

Overall, the scaling dimension of the Yukawa coupling is given by

$$\begin{aligned}
\dim[\Phi_s^a \sigma^a X^s \bar{\psi} \psi] &= 2 \dim[\psi] + \dim[\Phi] + \eta_{\text{vrtx}} \\
&= \frac{5}{2} + \frac{2}{9N_b \pi^2} - \frac{64}{3(N_f + 8N_b)\pi^2}.
\end{aligned} \tag{94}$$

The scaling dimension of the coupling constant  $y$  is thus

$$\dim[y] = \frac{1}{2} - \frac{2}{9N_b \pi^2} + \frac{64}{3(N_f + 8N_b)\pi^2}. \tag{95}$$

We observe that the fluctuations of the Lagrange multiplier act to reduce the scaling dimension of  $y$  (the second term on the right hand side of Eq. (95)), while the gauge field fluctuations act to increase the scaling dimension of  $y$  (the third term on the right hand side of Eq. (95)). This is to be contrasted with the result for the critical exponent  $\nu$  in Eq. (91), where both types of fluctuations decrease the value of  $\nu$ . The large flavor expansion is not expected to be a reliable estimate of the relative strength of the opposing tendencies in the renormalization of  $y$ , and so the ultimate fate of  $y$  at the SO(5) fixed point remains unclear. Evaluating Eq. (95) directly for the physically relevant  $N_f = 2, N_b = 2$  yields  $\approx 0.609 > 0$ .

As discussed in Sec. 2.5.2, there are additional symmetry-allowed fermion bilinears next to  $X^s = (\mu^z \gamma^x, \mu^x \gamma^y)$  for  $\Phi_{1,2}$  that can alter the form of the Yukawa coupling. Explicitly, they are given by  $\mu^x \gamma^x, \mu^z \gamma^y$ . As the  $\mu^a$  commute in both Eq. (92) and Eq. (93), they do not alter the logarithmic divergence and thus do not change the scaling dimension of  $y$ .

The relevance of the Yukawa coupling in the large- $N$  analysis implies that the SO(5)-symmetric fixed point is ultimately unstable in the strict infrared [32] and the relevant quantum field theory is the one studied in [27]. However, extensive numerical studies of deconfined criticality have demonstrated that weakly relevant perturbations can generate an extended regime of approximate SO(5) symmetry and scaling [33, 62], giving rise to pseudocritical or “walking” behavior [29, 36, 57]. In this regime, renormalization-group flows remain close to the SO(5)-symmetric fixed point over many decades before eventually running away, leading to apparent universal scaling with well-defined effective critical exponents [35]. From this perspective, the SO(5) fixed point acts as a controlling multicritical structure rather than a true infrared limit, reconciling the large- $N$  instability with numerical and experimental observations of robust deconfined-like behavior at intermediate scales [30, 53, 63–66].

## 4 Conclusion and Discussion

In this work, we have established a unified fermionic gauge-theory description of deconfined criticality on the square and Shastry–Sutherland lattices, demonstrating that their low-energy continuum theories coincide at the level of the most relevant couplings controlling Higgs transitions out of an  $SU(2)$   $\pi$ -flux parent state. Despite the reduced lattice symmetry of the Shastry–Sutherland geometry and the correspondingly enlarged set of symmetry-allowed fermion bilinears, we have shown that all such additional couplings are either irrelevant or share identical scaling dimensions with their square-lattice counterparts within a controlled large- $N$  expansion. As a result, the structure of the Higgs potential, the emergent  $SO(5)$  symmetry unifying Néel and valence-bond-solid order, and the leading operator content at criticality are preserved.

We have also proposed a candidate conformal field theory with  $SO(5)$  symmetry: a  $SU(2)$  gauge theory with  $N_f = 2$  massless, fundamental Dirac fermions, and  $N_b = 2$ , critical adjoint Higgs scalars. The  $N_f = 2$ ,  $N_b = 0$  case has been extensively studied earlier, with evidence for pseudo-critical behavior [29–35]. Adding  $N_b = 2$  adjoint Higgs scalars can reasonably be expected to stabilize the theory to a true conformal theory. This theory is proposed to control the physics near the boundary between the Néel and gapless  $\mathbb{Z}_2$  spin liquid states.

Our renormalization-group analysis identifies the Yukawa coupling between Dirac spinons and Higgs fields as the leading  $SO(5)$ -breaking perturbation, rendering the  $SO(5)$ -symmetric fixed point unstable at the lowest energies. Importantly, this instability is weak and naturally accounts for the growing body of numerical evidence indicating pseudocritical or “walking” behavior characterized by approximate  $SO(5)$  symmetry over an extended intermediate regime. Our results suggest that large anomalous dimensions of Néel and VBS order parameters may serve as a robust and experimentally relevant diagnostic of fermionic deconfined criticality, even when the ultimate infrared fixed point is unstable. This reinforces the view of the  $SO(5)$  theory as an organizing principle controlling extended pseudocritical regimes in frustrated quantum magnets. Taken together, our results place recent numerical observations of a gapless  $\mathbb{Z}_2$  Dirac spin liquid on the Shastry–Sutherland lattice within a coherent and controlled field-theoretic framework, and demonstrate that fermionic deconfined criticality extends beyond the square lattice to frustrated geometries with reduced symmetry.

Several directions emerge naturally from our analysis. First, while the present work establishes the operator content and leading instabilities of the  $SO(5)$  critical theory, a quantitative characterization of the associated pseudocritical regime—including crossover scales, finite-size scaling forms, and multifractal operator spectra—would provide a direct bridge to recent large-scale Monte Carlo studies. In this context, it would be particularly interesting to examine whether lattice-specific perturbations can parametrically enhance the extent of the walking regime on frustrated lattices relative to the square lattice.

Second, our framework can be generalized to incorporate additional symmetry-allowed perturbations such as Dzyaloshinskii–Moriya interactions, further-neighbor exchanges, or explicit breaking of spin-rotation symmetry, which are generically present in material realizations of the Shastry–Sutherland lattice. Understanding how such terms interact with the Higgs mechanism and the emergent gauge structure may shed light on the stability of gapless  $\mathbb{Z}_2$  spin liquids in realistic settings.

Third, the field theory developed here provides a natural starting point for studying dynamical probes and experimental signatures of fermionic deconfined criticality, including finite-temperature transport, dynamical structure factors, and responses to pressure or magnetic field in compounds such as  $SrCu_2(BO_3)_2$ . More broadly, our results suggest that fermionic deconfined criticality offers a unifying paradigm for organizing quantum phase transitions and proximate spin-liquid physics across a wide class of frustrated quantum magnets, motivating

its application to other lattices with reduced symmetry and complex unit cells.

Finally, from a field-theoretic perspective, several extensions of the present analysis are particularly natural. While our conclusions rely on a controlled large- $N$  expansion to determine operator relevance and stability, it would be valuable to complement this approach with alternative analytical techniques that are sensitive to finite- $N$  effects, such as conformal bootstrap methods applied to  $SO(5)$ -symmetric or weakly broken fixed points, or functional renormalization-group approaches that can capture runaway flows and walking behavior beyond leading order. Such methods may help quantify the extent to which the pseudocritical regime persists at physical values of  $N$  and clarify the nature of the eventual infrared fate.

In addition, the structure of the Majorana–Higgs theory suggests a broader landscape of nearby critical and multicritical points, including the possibility of tuning between distinct Higgs condensates or coupling multiple Higgs sectors. Exploring whether such extensions admit stable fixed points, complex fixed points, or lines of walking behavior may provide further insight into the universality and robustness of fermionic deconfined criticality. More generally, developing a systematic classification of allowed Higgs theories descending from  $SU(2)$   $\pi$ -flux states on lattices with reduced symmetry could help identify which aspects of deconfined criticality are truly universal and which depend sensitively on microscopic lattice structure.

**Funding information** This work is supported by the Deutsche Forschungsgemeinschaft (DFG, German Research Foundation) through Project-ID 258499086 – SFB 1170 and through the Würzburg-Dresden Cluster of Excellence on Complexity and Topology in Quantum Matter – ct.qmat Project-ID 390858490 – EXC 2147. The Flatiron Institute is a division of the Simons Foundation. S.S. was supported by the U.S. National Science Foundation grant No. DMR 2245246 and by the Simons Collaboration on Ultra-Quantum Matter which is a grant from the Simons Foundation (651440, S.S.). The work Y.I. was performed in part at the Aspen Center for Physics, which is supported by a grant from the Simons Foundation (1161654, Troyer). This research was also supported in part by grant NSF PHY-2309135 to the Kavli Institute for Theoretical Physics and by the International Centre for Theoretical Sciences (ICTS) for participating in the Discussion Meeting - Fractionalized Quantum Matter (code: ICTS/DMFQM2025/07). R.T. thanks IIT Madras for a Visiting Faculty Fellow position under the IoE program. Y.I. acknowledges support from the Abdus Salam International Centre for Theoretical Physics through the Associates Programme, from the Simons Foundation through Grant No. 284558FY19, from IIT Madras through the Institute of Eminence program for establishing QuCenDiEM (Project No. SP22231244CPETWOQCDHOC).

## A Projective symmetry group

In the following, we present details of the PSGs and *ansätze* for the SU(2)  $\pi$ -flux state, the U800 staggered-flux state, and the Z3000  $\mathbb{Z}_2$  state. These are based on the results of [22], but are presented here in a different gauge.

### A.1 SU(2) $\pi$ -flux

The PSG is given by

$$\begin{aligned} U_{T_{2x}}(\mathbf{r}, m_x, m_y) &= g_{T_{2x}}, \quad U_{T_{2y}}(\mathbf{r}, m_x, m_y) = g_{T_{2y}}, \\ U_{G_x}(\mathbf{r}, m_x, m_y) &= g_{G_x}, \\ U_{\sigma_{xy}}(\mathbf{r}, m_x, m_y) &= (-1)^{\delta_{(m_x, m_y), (B, B)}} g_{\sigma_{xy}}, \\ U_{\mathcal{T}}(\mathbf{r}, m_x, m_y) &= -(-1)^{\delta_{m_x, m_y}} g_{\mathcal{T}}, \end{aligned} \quad (\text{A.1})$$

where  $g_{T_{2x}}$ ,  $g_{T_{2y}}$ ,  $g_{G_x}$ ,  $g_{\sigma_{xy}}$  and  $g_{\mathcal{T}}$  are global SU(2) matrices. In this gauge, the structure of the *ansatz* is given by

$$u_{i, i+\hat{x}} = it, \quad u_{i, i+\hat{y}} = (-1)^{i_x} it. \quad (\text{A.2})$$

This *ansatz* also exists with square lattice symmetry and the associated PSG is given by:

$$\begin{aligned} U_{T_x}(\mathbf{i}) &= (-1)^{i_y} g_{T_x}, \quad U_{T_y}(\mathbf{i}) = g_{T_y}, \\ U_{P_x}(\mathbf{i}) &= (-1)^{i_x} g_{P_x}, \quad U_{P_y}(x, y) = (-1)^{i_y} g_{P_y}, \\ U_{R_{\pi/2}}(\mathbf{i}) &= (-1)^{i_x + i_x i_y} g_{R_{\pi/2}}, \\ U_{\mathcal{T}}(\mathbf{i}) &= (-1)^{i_x + i_y} g_{\mathcal{T}}. \end{aligned} \quad (\text{A.3})$$

### A.2 U800

The corresponding U(1) PSG can be obtained from Eq. (A.1) by choosing  $g_{T_{2x}} = e^{i\phi_{T_{2x}} \sigma^z}$ ,  $g_{T_{2y}} = e^{i\phi_{T_{2y}} \sigma^z}$ ,  $g_{G_x} = e^{i\phi_{G_x} \sigma^z} i\sigma^x$ ,  $g_{\sigma_{xy}} = e^{i\phi_{\sigma_{xy}} \sigma^z} i\sigma^x$  and  $g_{\mathcal{T}} = e^{i\phi_{\mathcal{T}} \sigma^z}$  and is given by:

$$\begin{aligned} U_{T_{2x}}(\mathbf{r}, m_x, m_y) &= e^{i\phi_{T_{2x}} \sigma^z}, \quad U_{T_{2y}}(\mathbf{r}, m_x, m_y) = e^{i\phi_{T_{2y}} \sigma^z}, \\ U_{G_x}(\mathbf{r}, m_x, m_y) &= e^{i\phi_{G_x} \sigma^z} i\sigma^x, \\ U_{\sigma_{xy}}(\mathbf{r}, m_x, m_y) &= (-1)^{\delta_{(m_x, m_y), (B, B)}} e^{i\phi_{\sigma_{xy}} \sigma^z} i\sigma^x, \\ U_{\mathcal{T}}(\mathbf{r}, m_x, m_y) &= -(-1)^{\delta_{m_x, m_y}} e^{i\phi_{\mathcal{T}} \sigma^z}. \end{aligned} \quad (\text{A.4})$$

where  $\phi \in [0, 2\pi)$ . In this gauge, the structure of the *ansatz* is given by:

$$\begin{aligned} u_{i, i+\hat{x}} &= it_{s,0} \sigma^0 - (-1)^{i_x + i_y} t_{s,z} \sigma^z, \\ u_{i, i+\hat{y}} &= (-1)^{i_x} it_{s,0} \sigma^0 + (-1)^{i_y} t_{s,z} \sigma^z. \end{aligned} \quad (\text{A.5})$$

In square lattice symmetry, the PSG is given by:

$$\begin{aligned} U_{T_x}(\mathbf{i}) &= (-1)^{i_y} e^{i\phi_{T_x} \sigma^z} i\sigma^x, \quad U_{T_y}(\mathbf{i}) = e^{i\phi_{T_y} \sigma^z} i\sigma^x, \\ U_{P_x}(\mathbf{i}) &= (-1)^{i_x} e^{i\phi_{P_x} \sigma^z}, \quad U_{P_y}(\mathbf{i}) = (-1)^{i_y} e^{i\phi_{P_y} \sigma^z}, \\ U_{R_{\pi/2}}(\mathbf{i}) &= (-1)^{i_x + i_x i_y} e^{i\phi_{R_{\pi/2}} \sigma^z} i\sigma^x, \\ U_{\mathcal{T}}(\mathbf{i}) &= (-1)^{i_x + i_y} e^{i\phi_{\mathcal{T}} \sigma^z}. \end{aligned} \quad (\text{A.6})$$

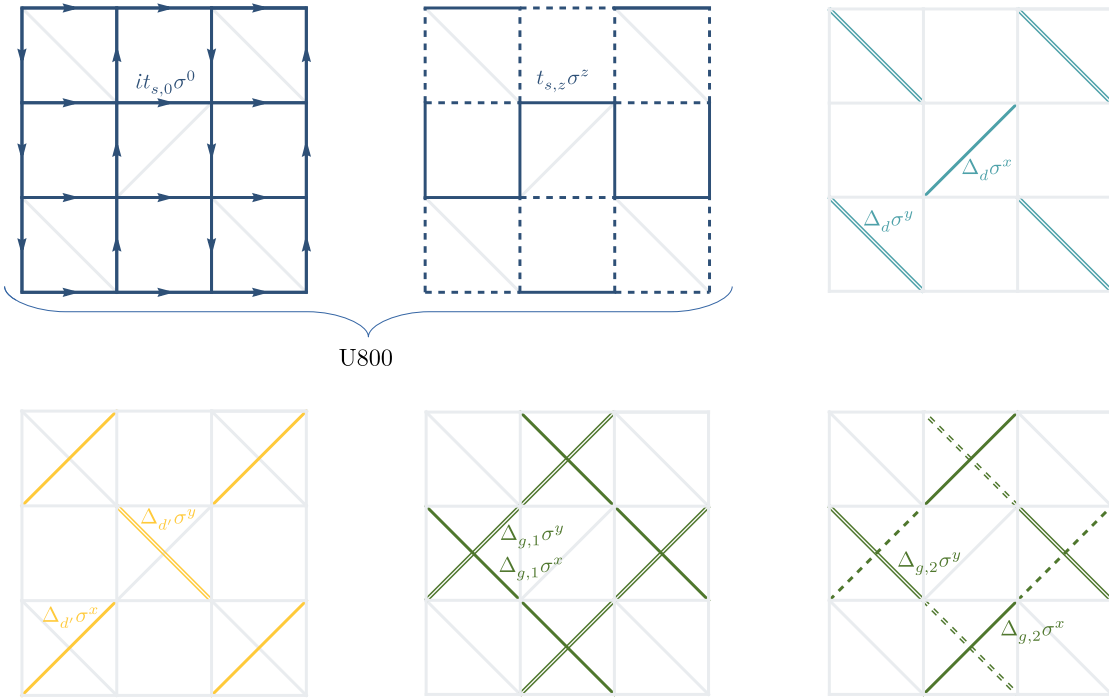


Figure 9: Sign structures of the hopping (also for U(1) *ansatz* labeled by U800) and pairing amplitudes of the  $\mathbb{Z}_2$  *ansatz* labeled by Z3000. For the staggered-flux structure  $(\varphi, -\varphi)$ , the hoppings are  $t_{s,0} = t \cos\left(\frac{\varphi-\pi}{4}\right)$  and  $t_{s,z} = t \sin\left(\frac{\varphi-\pi}{4}\right)$ . All the dashed links incorporate an additional negative sign.

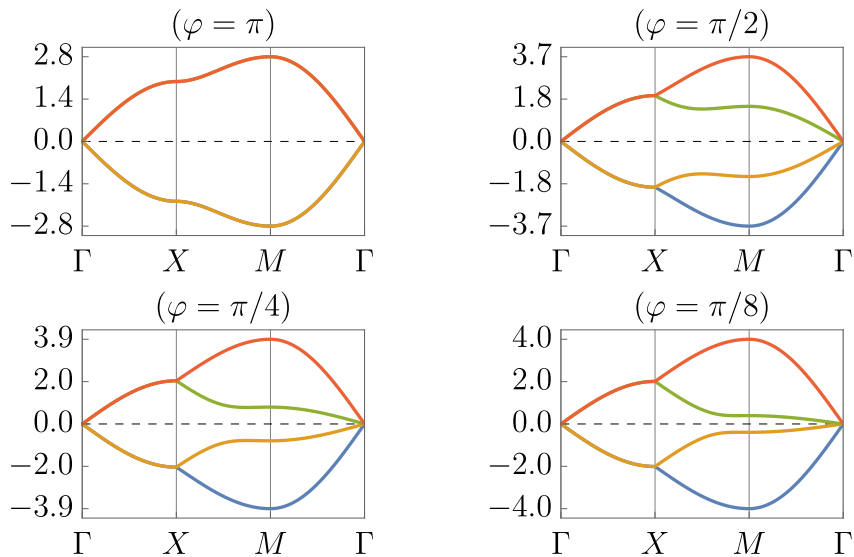


Figure 10: Spinon excitation spectra of U800 for different staggered fluxes  $\varphi$  along the high symmetry paths connecting the high-symmetry points given  $\Gamma(0, 0)$ ,  $X(\frac{\pi}{2}, 0)$  and  $M(\frac{\pi}{2}, \frac{\pi}{2})$ .

The dispersion of U800 for different parameters of  $\phi$  is shown in Fig. 10 showing 4 Dirac points at the  $\Gamma$  point.

### A.3 Z3000

The corresponding  $\mathbb{Z}_2$  PSG can be obtained from Eq. (A.4) by choosing  $\phi_{T_{2x}} = \phi_{T_{2y}} = 0$ ,  $\phi_{G_x} = -\pi/4$ ,  $\phi_{\sigma_{xy}} = -\pi/2$ , and  $\phi_{\mathcal{T}} = \pi/2$  and is given by

$$\begin{aligned} U_{T_{2x}}(\mathbf{r}, m_x, m_y) &= U_{T_{2y}}(\mathbf{r}, m_x, m_y) = \sigma^0, \\ U_{G_x}(\mathbf{r}, m_x, m_y) &= i \frac{1}{\sqrt{2}} (\sigma^x + \sigma^y), \\ U_{\sigma_{xy}}(\mathbf{r}, m_x, m_y) &= (-1)^{\delta_{(m_x, m_y), (BB)}} i \sigma^y, \\ U_{\mathcal{T}}(\mathbf{r}, m_x, m_y) &= -(-1)^{\delta_{m_x, m_y}} i \sigma^z. \end{aligned} \quad (\text{A.7})$$

In this gauge, the structure of the *ansatz* is given by Eqs. (8)-(17). Figure 9 illustrates the sign structures of the mean-field hopping and pairing amplitudes of the descendant  $\mathbb{Z}_2$  *ansatz* labeled by Z3000 (which is also connected to Z2Azz13 on the square lattice). Notice that in the illustrated gauge form, the connection to the parent U(1) state U800 is explicit as the removal of the pairing terms gives the parent state.

## B Perturbations due to pairing terms

In this Appendix, we present details on the derivation of the perturbations due to the pairing terms  $\Delta_{g,1/2}$ :

$$\begin{aligned} \delta H &= \sum_{\mathbf{r}} \text{Tr} \left\{ (\Delta_{g,1} \sigma^y - \Delta_{g,2} \sigma^x) [\mathcal{X}_{\mathbf{r},A,0}^\dagger + \mathcal{X}_{\mathbf{r},B,1}^\dagger] [\mathcal{X}_{\mathbf{r}+\hat{\mathbf{x}},B,0} - \mathcal{X}_{\mathbf{r}+\hat{\mathbf{x}},A,1}] + \text{h.c.} \right. \\ &\quad + (\Delta_{g,1} \sigma^x + \Delta_{g,2} \sigma^y) [\mathcal{X}_{\mathbf{r},B,0}^\dagger + \mathcal{X}_{\mathbf{r},A,1}^\dagger] [\mathcal{X}_{\mathbf{r}-\hat{\mathbf{x}},A,0} - \mathcal{X}_{\mathbf{r}-\hat{\mathbf{x}},B,1}] + \text{h.c.} \\ &\quad + (\Delta_{g,1} \sigma^y + \Delta_{g,2} \sigma^x) [\mathcal{X}_{\mathbf{r},B,0}^\dagger - \mathcal{X}_{\mathbf{r},A,1}^\dagger] [\mathcal{X}_{\mathbf{r}+\hat{\mathbf{y}},A,0} + \mathcal{X}_{\mathbf{r}+\hat{\mathbf{y}},B,1}] + \text{h.c.} \\ &\quad \left. + (\Delta_{g,1} \sigma^x - \Delta_{g,2} \sigma^y) [\mathcal{X}_{\mathbf{r},A,0}^\dagger - \mathcal{X}_{\mathbf{r},B,1}^\dagger] [\mathcal{X}_{\mathbf{r}+\hat{\mathbf{y}},B,0} + \mathcal{X}_{\mathbf{r}+\hat{\mathbf{y}},A,1}] + \text{h.c.} \right\} \\ &\approx \int d^2 \mathbf{r} \text{Tr} \left\{ (\Delta_{g,1} \sigma^y - \Delta_{g,2} \sigma^x) (\mathcal{X}^\dagger \rho^x \mu^z \mathcal{X} - \mathcal{X}^\dagger \rho^z \mu^x \mathcal{X}) \right. \\ &\quad + (\Delta_{g,1} \sigma^x + \Delta_{g,2} \sigma^y) (\mathcal{X}^\dagger \rho^x \mu^z \mathcal{X} + \mathcal{X}^\dagger \rho^z \mu^x \mathcal{X}) \\ &\quad + (\Delta_{g,1} \sigma^y + \Delta_{g,2} \sigma^x) (\mathcal{X}^\dagger \rho^x \mu^z \mathcal{X} - \mathcal{X}^\dagger \rho^z \mu^x \mathcal{X}) \\ &\quad \left. + (\Delta_{g,1} \sigma^x - \Delta_{g,2} \sigma^y) (\mathcal{X}^\dagger \rho^x \mu^z \mathcal{X} + \mathcal{X}^\dagger \rho^z \mu^x \mathcal{X}) \right\} \\ \Rightarrow \delta \mathcal{L} &= 2\Delta_{g,1} \text{Tr}[\sigma^x \bar{\mathcal{X}} (\gamma^x \mu^z - \gamma^y \mu^x) \mathcal{X}] + 2\Delta_{g,1} \text{Tr}[\sigma^y \bar{\mathcal{X}} (\gamma^x \mu^z + \gamma^y \mu^x) \mathcal{X}]. \end{aligned} \quad (\text{B.1})$$

As we can see, to lowest order  $\Delta_{g,2}$  vanishes, but there is non-vanishing gradient term, which we now extract:

$$\begin{aligned}
\delta_H = & \sum_r \Delta_{g,2} \text{Tr} \left\{ \sigma^x [\mathcal{X}_{r,A,0}^\dagger + \mathcal{X}_{r,B,1}^\dagger] [\mathcal{X}_{r-\hat{y},B,0} - \mathcal{X}_{r-\hat{y},A,1}] + [\mathcal{X}_{r,B,0}^\dagger - \mathcal{X}_{r,A,1}^\dagger] [\mathcal{X}_{r+\hat{y},A,0} + \mathcal{X}_{r+\hat{y},B,1}] \right. \\
& \quad \left. - [\mathcal{X}_{r,A,0}^\dagger + \mathcal{X}_{r,B,1}^\dagger] [\mathcal{X}_{r+\hat{x},B,0} - \mathcal{X}_{r+\hat{x},A,1}] - [\mathcal{X}_{r,B,0}^\dagger - \mathcal{X}_{r,A,1}^\dagger] [\mathcal{X}_{r-\hat{x},A,0} + \mathcal{X}_{r-\hat{x},B,1}] \right\} \\
& + \Delta_{g,2} \text{Tr} \left\{ \sigma^y [\mathcal{X}_{r,B,0}^\dagger + \mathcal{X}_{r,A,1}^\dagger] [\mathcal{X}_{r-\hat{x},A,0} - \mathcal{X}_{r-\hat{x},B,1}] + [\mathcal{X}_{r,A,0}^\dagger - \mathcal{X}_{r,B,1}^\dagger] [\mathcal{X}_{r+\hat{x},B,0} + \mathcal{X}_{r+\hat{x},A,1}] \right. \\
& \quad \left. - [\mathcal{X}_{r,B,0}^\dagger + \mathcal{X}_{r,A,1}^\dagger] [\mathcal{X}_{r-\hat{y},A,0} - \mathcal{X}_{r-\hat{y},B,1}] - [\mathcal{X}_{r,A,0}^\dagger - \mathcal{X}_{r,B,1}^\dagger] [\mathcal{X}_{r+\hat{y},B,0} + \mathcal{X}_{r+\hat{y},A,1}] \right\} \\
\approx & \Delta_{g,2} \int d^2 r \text{Tr} \{ \sigma^x \mathcal{X}^\dagger (\mu^y - \rho^y) (i\partial_x + i\partial_y) \mathcal{X} \} + \text{Tr} \{ \sigma^x \mathcal{X}^\dagger (-\mu^y - \rho^y) (i\partial_y - i\partial_x) \mathcal{X} \} \\
\Rightarrow \delta \mathcal{L} = & \Delta_{g,2} \text{Tr} [\sigma^x \bar{\mathcal{X}} (-\gamma^0 \mu^y + 1) (i\partial_x + i\partial_y) \mathcal{X} + \sigma^y \bar{\mathcal{X}} (i\gamma^0 \mu^y + 1) (i\partial_y - i\partial_x) \mathcal{X}].
\end{aligned} \tag{B.2}$$

## C Saddle point expansion

We present more details on the derivation of the expansion of the free energy around the saddle point up to second order. In the bosonic sector, we obtain the corrections

$$\begin{aligned}
N_b \int \frac{d^3 p}{(2\pi)^3} \frac{d^3 q}{(2\pi)^3} \left( 8G_\Phi(q) \delta_{p,0} \int \frac{d^3 p'}{(2\pi)^3} A_\mu^a(p') A_\mu^a(-p') \right. \\
\left. - \frac{1}{2} G_\Phi(q) G_\Phi(q-p) \left[ -3\lambda(p)\lambda(-p) + 8(2q-p)_\mu A_\mu^a(p)(2q-p)_\nu A_\nu^a(-p) \right] \right)
\end{aligned} \tag{C.1}$$

and in the fermionic sector

$$-\frac{N_f}{2} \int \frac{d^3 p}{(2\pi)^3} \frac{d^3 q}{(2\pi)^3} \text{Tr} [G_\psi(q) \gamma^\mu A_\mu^a(p) \sigma_a G_\psi(p+q) \gamma^\nu A_\nu^b(-p) \sigma_b]. \tag{C.2}$$

The diagrams corresponding to these terms are shown in Fig. 11. These integrals are identical to [26], and the results are:

$$\int \frac{d^3 q}{(2\pi)^3} \frac{1}{q^2 + r} = -\frac{\sqrt{r}}{4\pi}, \tag{C.3}$$

$$\int \frac{d^3 q}{(2\pi)^3} \frac{1}{(q^2 + r)((q-p)^2 + r)} = \frac{1}{4\pi p} \arctan \frac{p}{2\sqrt{r}}, \tag{C.4}$$

$$\begin{aligned}
\int \frac{d^3 q}{(2\pi)^3} \frac{(2q-p)_\mu (2q-p)_\nu}{(q^2 + r)((q-p)^2 + r)} = & - \left( \delta_{\mu\nu} + \frac{p_\mu p_\nu}{p^2} \right) \frac{\sqrt{r}}{4\pi} \\
& - \left( \delta_{\mu\nu} - \frac{p_\mu p_\nu}{p^2} \right) \left( \frac{4r + p^2}{8\pi p} \arctan \frac{p}{2\sqrt{r}} \right),
\end{aligned} \tag{C.5}$$

$$\int \frac{d^3 q}{(2\pi)^3} \frac{\text{Tr} [\gamma^\mu q \gamma^\nu (p+q)]}{q^2 (p+q)^2} = -\frac{1}{16p}. \tag{C.6}$$

## D Useful integrals

In this Appendix, we exemplify the extraction of the logarithmic divergences via dimensional regularization for some of the integrals which appear in our treatment.

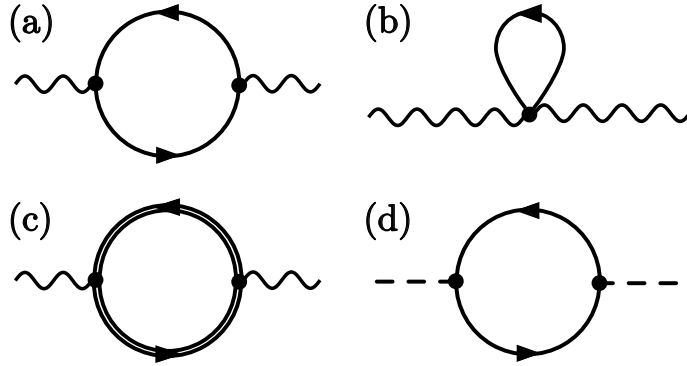


Figure 11: One-loop diagrams that determine the effective action at large  $N_f$  and  $N_b$ . (a), (b) and (c) contribute to the effective action for the  $A_\mu$  and (d) contributes to the action of the  $\lambda$  field.

### D.1 Fermion self-energy

We can calculate the Fermion self-energy Eq. (64) as

$$\begin{aligned}
 \Sigma_\psi(k) &= \sigma^a \sigma^a \int \frac{d^3 q}{(2\pi)^3} \gamma_\mu G_\psi(k+q) \gamma_\nu D_{\mu\nu}(-q) \\
 &= 3 \int \frac{d^3 q}{(2\pi)^3} \frac{16}{N_f + 8N_b} \gamma_\mu \frac{q + \not{k}}{(k+q)^2} \gamma_\nu \frac{1}{q} (\delta_{\mu\nu} - \zeta \frac{q_\mu q_\nu}{q^2}) \\
 &= 3 \frac{16}{N_f + 8N_b} \int \frac{d^3 q}{(2\pi)^3} \left[ \gamma_\mu \frac{q + \not{k}}{(k+q)^2 q} \gamma_\nu - \zeta \frac{q(q + \not{k})q}{(k+q)^2 q^3} \right] \\
 &= 3 \frac{16}{N_f + 8N_b} \int \frac{d^3 q}{(2\pi)^3} \left[ -\frac{q + \not{k}}{(k+q)^2 q} + \zeta \frac{q(q + \not{k})q}{(k+q)^2 q^3} \right].
 \end{aligned} \tag{D.1}$$

We split the integral in two parts. We solve each by dimensional regularization by introducing a Feynman parameter  $x$  and defining  $l = q + (1-x)k$ :

$$\begin{aligned}
 \int \frac{d^3 q}{(2\pi)^3} \frac{q + \not{k}}{(k+q)^2 q} &= \frac{1}{2} \int_0^1 dx \int \frac{d^3 q}{(2\pi)^3} \frac{x^{-1/2} (q + \not{k})}{[(1-x)(k+q)^2 + xq^2]^{3/2}} \\
 &= \frac{1}{2} \int_0^1 dx \int \frac{d^3 l}{(2\pi)^3} \frac{x^{-1/2} (l + x\not{k})}{[l^2 + x(1-x)k^2]^{3/2}} \\
 &= \int_0^1 dx \frac{1}{2(4\pi)^{3/2}} \left[ \frac{\sqrt{x}\not{k}}{\Gamma(3/2)} \frac{\Gamma(0)}{[x(1-x)k^2]^{10}} \right] \\
 &\rightarrow -\frac{1}{6\pi^2} \not{k} \log k
 \end{aligned} \tag{D.2}$$

In the last line, we performed the dimensional regularization in the following way: Define  $\Delta = x(1-x)k^2$  and  $\epsilon = \frac{D}{2} - \frac{3}{2}$ , then

$$\frac{\Gamma(\epsilon)}{\Delta^\epsilon} \approx \frac{1/\epsilon}{1 + \epsilon \log \Delta} \approx \frac{1}{\epsilon} - \log \Delta \rightarrow -\log k^2 = -2 \log k. \tag{D.3}$$

The second integral similarly gives

$$\begin{aligned}
\int \frac{d^3 q}{(2\pi)^3} \frac{q(q+k)q}{(k+q)^2 q^3} &= \frac{3}{2} \int_0^1 dx \int \frac{d^3 q}{(2\pi)^3} \frac{\sqrt{x}q(q+k)q}{[(1-x)(k+q)+xq^2]^{5/2}} \\
&= \frac{3}{2} \int_0^1 dx \sqrt{x} \int \frac{d^3 l}{(2\pi)^3} \frac{(l-(1-x)k)(l+xk)(l-(1-x)k)}{[l^2+x(1-x)k^2]^{5/2}} \\
&\rightarrow \frac{3}{2} \int_0^1 dx \frac{\sqrt{x}(-2\log k)}{8\pi\sqrt{\pi}\cdot 2\Gamma(5/2)} \delta_{\mu\nu} \left[ -(1-x)(\gamma^\mu\gamma^\nu k + k\gamma^\mu\gamma^\nu) + x\gamma^\mu k\gamma^\nu \right] \\
&= \int_0^1 dx \frac{-2\sqrt{x}\log k}{8\pi^2} \left[ -3(1-x)k - xk - 3(1-x)k \right] \\
&= \int_0^1 dx \frac{-2\sqrt{x}(5x-6)}{8\pi^2} k \log k \\
&= -\frac{1}{2\pi^2} k \log k.
\end{aligned} \tag{D.4}$$

## D.2 Boson self-energy

The boson self-energy corrections in Eq. (68) read

$$\begin{aligned}
I_{A;1} &= 8 \int \frac{d^3 q}{(2\pi)^3} G_\Phi(k+q) D_{\mu\nu}(-q) (2k+q)_\mu (2k+q)_\nu \\
&= \frac{8 \cdot 16}{N_f + 8N_b} \int \frac{d^3 q}{(2\pi)^3} \frac{(2k+q)_\mu (2k+q)_\nu}{q(k+q)^2} \left( \delta_{\mu\nu} - \zeta \frac{q_\mu q_\nu}{q^2} \right) \\
&= \frac{8 \cdot 16}{N_f + 8N_b} \int \frac{d^3 q}{(2\pi)^3} \left[ \frac{(2k+q)^2}{q(k+q)^2} - \zeta \frac{(2kq+q^2)^2}{q^3(k+q)^2} \right].
\end{aligned} \tag{D.5}$$

We solve both integrals:

$$\begin{aligned}
\int \frac{d^3 q}{(2\pi)^3} \frac{(2k+q)^2}{q(k+q)^2} &= \frac{1}{2} \int_0^1 dx \int \frac{d^3 q}{(2\pi)^3} \frac{x^{-1/2}(2k+q)^2}{[(1-x)(k+q)^2+xq^2]^{3/2}} \\
&= \frac{1}{2} \int_0^1 dx \int \frac{d^3 l}{(2\pi)^3} \frac{x^{-1/2}(l+(1+x)k)^2}{[l^2+x(1-x)k^2]^{3/2}} \\
&\rightarrow \frac{k^2 \log k}{16\pi\sqrt{\pi}\Gamma(3/2)} \int_0^1 dx \frac{1}{\sqrt{x}} \left[ -2(1+x)^2 + 3x(1-x) \right] \\
&= -\frac{10}{12\pi^2} k^2 \log k.
\end{aligned} \tag{D.6}$$

$$\begin{aligned}
\int \frac{d^3q}{(2\pi)^3} \frac{(2kq+q^2)^2}{q^3(k+q)^2} &= \frac{3}{2} \int_0^1 dx \int \frac{d^3q}{(2\pi)^3} \frac{\sqrt{x}(2kq+q^2)^2}{[(1-x)(k+q)^2+xq^2]^{5/2}} \\
&= \frac{3}{2} \int_0^1 dx \int \frac{d^3l}{(2\pi)^3} \frac{\sqrt{x}[(l+(1+x)k)_\mu(l-(1-x)k)_\mu]^2}{[l^2+x(1-x)k^2]^{5/2}} \\
&= \frac{3}{2} \int_0^1 dx \sqrt{x} \int \frac{d^3l}{(2\pi)^3} \frac{(l^2)^2+4x^2(k \cdot l)^2+(1-x^2)^2k^4-2(1-x^2)l^2k^2}{[l^2+x(1-x)k^2]^{5/2}} \\
&\rightarrow \frac{3}{2} \frac{k^2 \log k}{8\pi\sqrt{\pi}\Gamma(5/2)} \int_0^1 dx \sqrt{x} \left[ \frac{15x(1-x)}{2} - 4x^2 + 6(1-x^2) \right] \\
&= \frac{1}{2\pi^2} k^2 \log k.
\end{aligned} \tag{D.7}$$

The Lagrange multiplier fluctuations contribute [Eq. (70)]:

$$\begin{aligned}
I_{\lambda;1} &= i^2 \int \frac{d^3q}{(2\pi)^3} G_\Phi(k+q) D_\lambda(-q) \\
&= -\frac{8}{3N_b} \int \frac{d^3q}{(2\pi)^3} \frac{q^2}{q(k+q)^2} \\
&= -\frac{4}{3N_b} \int_0^1 dx \int \frac{d^3q}{(2\pi)^3} \frac{x^{-1/2}q^2}{[(1-x)(k+q)^2+xq^2]^{3/2}} \\
&= -\frac{4}{3N_b} \int_0^1 dx \int \frac{d^3l}{(2\pi)^3} x^{-1/2} \frac{l^2+(1-x)^2k^2-2(1-x)l \cdot k}{[l^2+x(1-x)k^2]^{3/2}} \\
&\rightarrow -\frac{4}{3N_b \cdot 8\pi\sqrt{\pi}\Gamma(3/2)} \int_0^1 dx \frac{1}{\sqrt{x}} \left[ \frac{6x(1-x)}{2} - 2(1-x)^2 \right] k^2 \log k \\
&= \frac{4}{9N_b\pi^2} k^2 \log k.
\end{aligned} \tag{D.8}$$

### D.3 SO(5) vertex corrections

The vertex correction due to the gauge field is given by

$$\begin{aligned}
I_{A;2} &= 3 \int \frac{d^3q}{(2\pi)^3} \gamma_\mu G_\psi(k_1+q) G_\psi(k_2+q) \gamma_\nu D_{\mu\nu}(-q) \\
&= \frac{3 \cdot 16}{N_f + 8N_b} \int \frac{d^3q}{(2\pi)^3} \gamma_\mu \frac{\not{k}_1 + \not{q}}{(k_1+q)^2} \frac{\not{k}_2 + \not{q}}{(k_2+q)^2} \frac{1}{q} \gamma_\nu \left( \delta_{\mu\nu} - \zeta \frac{q_\mu q_\nu}{q^2} \right) \\
&= \frac{3 \cdot 16}{N_f + 8N_b} \int \frac{d^3q}{(2\pi)^3} \left[ \frac{-(\not{k}_1 + \not{q})(\not{k}_2 + \not{q}) + 4(k_1+q) \cdot (k_2+q)}{(k_1+q)^2(k_2+q)^2 q} - \zeta \frac{\not{q}(\not{k}_1 + \not{q})(\not{k}_2 + \not{q})q}{(k_1+q)^2(k_2+q)^2 q^3} \right].
\end{aligned} \tag{D.9}$$

We will now focus on the case  $k_1 = k_2 \equiv k$ . We split the integral into 2 parts and solve each of them via dimensional regularization:

$$\begin{aligned}
 I_{A;2,1} &= \int \frac{d^3q}{(2\pi)^3} \frac{3}{(k+q)^2 q} \\
 &= \frac{1}{2} \int_0^1 dx \int \frac{d^3q}{(2\pi)^3} \frac{3x^{-1/2}}{[(1-x)(k+q)^2 + xq^2]^{3/2}} \\
 &= \frac{3}{2} \int_0^1 dx \frac{1}{\sqrt{x}} \int \frac{d^3l}{(2\pi)^3} \frac{1}{[l^2 + x(1-x)k^2]^{3/2}} \\
 &\rightarrow \frac{3}{2} \int_0^1 dx \frac{1}{\sqrt{x}} \frac{1}{8\pi\sqrt{\pi}\Gamma(3/2)} (-2\log k) = \frac{-3i}{2\pi^2} \log k,
 \end{aligned} \tag{D.10}$$

and

$$I_{A;2,2} = \int \frac{d^3q}{(2\pi)^3} \frac{q^2}{(k+q)^2 q^3} = \frac{1}{3} I_{A;2,1}. \tag{D.11}$$

## References

- [1] T. Senthil, A. Vishwanath, L. Balents, S. Sachdev and M. P. A. Fisher, *Deconfined Quantum Critical Points*, *Science* **303**(5663), 1490 (2004), doi:[10.1126/science.1091806](https://doi.org/10.1126/science.1091806).
- [2] T. Senthil, L. Balents, S. Sachdev, A. Vishwanath and M. P. A. Fisher, *Quantum criticality beyond the Landau-Ginzburg-Wilson paradigm*, *Phys. Rev. B* **70**, 144407 (2004), doi:[10.1103/PhysRevB.70.144407](https://doi.org/10.1103/PhysRevB.70.144407).
- [3] A. W. Sandvik, *Evidence for Deconfined Quantum Criticality in a Two-Dimensional Heisenberg Model with Four-Spin Interactions*, *Phys. Rev. Lett.* **98**, 227202 (2007), doi:[10.1103/PhysRevLett.98.227202](https://doi.org/10.1103/PhysRevLett.98.227202).
- [4] M. Hermele, T. Senthil and M. P. A. Fisher, *Algebraic spin liquid as the mother of many competing orders*, *Phys. Rev. B* **72**, 104404 (2005), doi:[10.1103/PhysRevB.72.104404](https://doi.org/10.1103/PhysRevB.72.104404).
- [5] P. A. Lee, N. Nagaosa and X.-G. Wen, *Doping a Mott insulator: Physics of high-temperature superconductivity*, *Rev. Mod. Phys.* **78**, 17 (2006), doi:[10.1103/RevModPhys.78.17](https://doi.org/10.1103/RevModPhys.78.17).
- [6] X.-Y. Song, Y.-C. He, A. Vishwanath and C. Wang, *From Spinon Band Topology to the Symmetry Quantum Numbers of Monopoles in Dirac Spin Liquids*, *Phys. Rev. X* **10**, 011033 (2020), doi:[10.1103/PhysRevX.10.011033](https://doi.org/10.1103/PhysRevX.10.011033).
- [7] I. Affleck and J. B. Marston, *Large- $n$  limit of the Heisenberg-Hubbard model: Implications for high- $T_c$  superconductors*, *Phys. Rev. B* **37**, 3774 (1988), doi:[10.1103/PhysRevB.37.3774](https://doi.org/10.1103/PhysRevB.37.3774).
- [8] X.-G. Wen, *Quantum orders and symmetric spin liquids*, *Phys. Rev. B* **65**, 165113 (2002), doi:[10.1103/PhysRevB.65.165113](https://doi.org/10.1103/PhysRevB.65.165113).
- [9] M. Hermele, T. Senthil, M. P. A. Fisher, P. A. Lee, N. Nagaosa and X.-G. Wen, *Stability of  $U(1)$  spin liquids in two dimensions*, *Phys. Rev. B* **70**, 214437 (2004), doi:[10.1103/PhysRevB.70.214437](https://doi.org/10.1103/PhysRevB.70.214437).

[10] M. Hermele, *SU(2) gauge theory of the Hubbard model and application to the honeycomb lattice*, Phys. Rev. B **76**, 035125 (2007), doi:[10.1103/PhysRevB.76.035125](https://doi.org/10.1103/PhysRevB.76.035125).

[11] N. Read and S. Sachdev, *Large- $N$  expansion for frustrated quantum antiferromagnets*, Phys. Rev. Lett. **66**, 1773 (1991), doi:[10.1103/PhysRevLett.66.1773](https://doi.org/10.1103/PhysRevLett.66.1773).

[12] S. Sachdev and R. Jalabert, *Effective Lattice Models for Two-Dimensional Quantum Antiferromagnets*, Mod. Phys. Lett. B **04**(16), 1043 (1990), doi:[10.1142/S0217984990001318](https://doi.org/10.1142/S0217984990001318).

[13] A. Tanaka and X. Hu, *Many-Body Spin Berry Phases Emerging from the  $\pi$ -Flux State: Competition between Antiferromagnetism and the Valence-Bond-Solid State*, Phys. Rev. Lett. **95**, 036402 (2005), doi:[10.1103/PhysRevLett.95.036402](https://doi.org/10.1103/PhysRevLett.95.036402).

[14] T. Senthil and M. P. A. Fisher, *Competing orders, nonlinear sigma models, and topological terms in quantum magnets*, Phys. Rev. B **74**, 064405 (2006), doi:[10.1103/PhysRevB.74.064405](https://doi.org/10.1103/PhysRevB.74.064405).

[15] A. Thomson and S. Sachdev, *Fermionic Spinon Theory of Square Lattice Spin Liquids near the Néel State*, Phys. Rev. X **8**, 011012 (2018), doi:[10.1103/PhysRevX.8.011012](https://doi.org/10.1103/PhysRevX.8.011012).

[16] B. Sriram Shastry and B. Sutherland, *Exact ground state of a quantum mechanical antiferromagnet*, Physica B+C **108**(1), 1069 (1981), doi:[https://doi.org/10.1016/0378-4363\(81\)90838-X](https://doi.org/10.1016/0378-4363(81)90838-X).

[17] J. Yang, A. W. Sandvik and L. Wang, *Quantum criticality and spin liquid phase in the Shastry-Sutherland model*, Phys. Rev. B **105**, L060409 (2022), doi:[10.1103/PhysRevB.105.L060409](https://doi.org/10.1103/PhysRevB.105.L060409).

[18] L. Wang, Y. Zhang and A. W. Sandvik, *Quantum Spin Liquid Phase in the Shastry-Sutherland Model Detected by an Improved Level Spectroscopic Method*, Chin. Phys. Lett. **39**(7), 077502 (2022), doi:[10.1088/0256-307X/39/7/077502](https://doi.org/10.1088/0256-307X/39/7/077502).

[19] L. L. Viteritti, R. Rende, A. Parola, S. Goldt and F. Becca, *Transformer wave function for two dimensional frustrated magnets: Emergence of a spin-liquid phase in the Shastry-Sutherland model*, Phys. Rev. B **111**, 134411 (2025), doi:[10.1103/PhysRevB.111.134411](https://doi.org/10.1103/PhysRevB.111.134411).

[20] A. Keleş and E. Zhao, *Rise and fall of plaquette order in the Shastry-Sutherland magnet revealed by pseudofermion functional renormalization group*, Phys. Rev. B **105**, L041115 (2022), doi:[10.1103/PhysRevB.105.L041115](https://doi.org/10.1103/PhysRevB.105.L041115).

[21] P. Corboz, Y. Zhang, B. Ponsioen and F. Mila, *Quantum spin liquid phase in the Shastry-Sutherland model revealed by high-precision infinite projected entangled-pair states* (2025), [2502.14091](https://arxiv.org/abs/2502.14091).

[22] A. Maity, F. Ferrari, J. Y. Lee, J. Potten, T. Müller, R. Thomale, R. Samajdar and Y. Iqbal, *Evidence for a  $\mathbb{Z}_2$  Dirac spin liquid in the generalized Shastry-Sutherland model* (2024), [2501.00096](https://arxiv.org/abs/2501.00096).

[23] I. Affleck, Z. Zou, T. Hsu and P. W. Anderson, *SU(2) gauge symmetry of the large- $U$  limit of the Hubbard model*, Phys. Rev. B **38**, 745 (1988), doi:[10.1103/PhysRevB.38.745](https://doi.org/10.1103/PhysRevB.38.745).

[24] E. Dagotto, E. Fradkin and A. Moreo, *SU(2) gauge invariance and order parameters in strongly coupled electronic systems*, Phys. Rev. B **38**, 2926 (1988), doi:[10.1103/PhysRevB.38.2926](https://doi.org/10.1103/PhysRevB.38.2926).

[25] X.-G. Wen and P. A. Lee, *Theory of Underdoped Cuprates*, Phys. Rev. Lett. **76**(3), 503 (1996), doi:[10.1103/PhysRevLett.76.503](https://doi.org/10.1103/PhysRevLett.76.503), cond-mat/9506065.

[26] M. Christos, L. Shackleton, S. Sachdev and Z.-X. Luo, *Deconfined quantum criticality of nodal d-wave superconductivity, Néel order, and charge order on the square lattice at half-filling*, Phys. Rev. Res. **6**, 033018 (2024), doi:[10.1103/PhysRevResearch.6.033018](https://doi.org/10.1103/PhysRevResearch.6.033018).

[27] L. Shackleton, A. Thomson and S. Sachdev, *Deconfined criticality and a gapless  $\mathbb{Z}_2$  spin liquid in the square-lattice antiferromagnet*, Phys. Rev. B **104**, 045110 (2021), doi:[10.1103/PhysRevB.104.045110](https://doi.org/10.1103/PhysRevB.104.045110).

[28] L. Shackleton and S. Sachdev, *Anisotropic deconfined criticality in Dirac spin liquids*, JHEP **07**, 141 (2022), doi:[10.1007/JHEP07\(2022\)141](https://doi.org/10.1007/JHEP07(2022)141), 2203.01962.

[29] A. Nahum, P. Serna, J. T. Chalker, M. Ortúñoz and A. M. Somoza, *Emergent  $SO(5)$  Symmetry at the Néel to Valence-Bond-Solid Transition*, Phys. Rev. Lett. **115**, 267203 (2015), doi:[10.1103/PhysRevLett.115.267203](https://doi.org/10.1103/PhysRevLett.115.267203).

[30] C. Wang, A. Nahum, M. A. Metlitski, C. Xu and T. Senthil, *Deconfined Quantum Critical Points: Symmetries and Dualities*, Phys. Rev. X **7**, 031051 (2017), doi:[10.1103/PhysRevX.7.031051](https://doi.org/10.1103/PhysRevX.7.031051).

[31] Z. Wang, M. P. Zaletel, R. S. K. Mong and F. F. Assaad, *Phases of the (2 + 1) Dimensional  $SO(5)$  Nonlinear Sigma Model with Topological Term*, Phys. Rev. Lett. **126**, 045701 (2021), doi:[10.1103/PhysRevLett.126.045701](https://doi.org/10.1103/PhysRevLett.126.045701).

[32] Z. Zhou, L. Hu, W. Zhu and Y.-C. He,  *$SO(5)$  Deconfined Phase Transition under the Fuzzy-Sphere Microscope: Approximate Conformal Symmetry, Pseudo-Criticality, and Operator Spectrum*, Phys. Rev. X **14**, 021044 (2024), doi:[10.1103/PhysRevX.14.021044](https://doi.org/10.1103/PhysRevX.14.021044).

[33] B.-B. Chen, X. Zhang, Y. Wang, K. Sun and Z. Y. Meng, *Phases of (2+1)D  $SO(5)$  Nonlinear Sigma Model with a Topological Term on a Sphere: Multicritical Point and Disorder Phase*, Phys. Rev. Lett. **132**, 246503 (2024), doi:[10.1103/PhysRevLett.132.246503](https://doi.org/10.1103/PhysRevLett.132.246503).

[34] B.-B. Chen, X. Zhang and Z. Y. Meng, *Emergent conformal symmetry at the multicritical point of (2 + 1)D  $SO(5)$  model with Wess-Zumino-Witten term on a sphere*, Phys. Rev. B **110**, 125153 (2024), doi:[10.1103/PhysRevB.110.125153](https://doi.org/10.1103/PhysRevB.110.125153).

[35] J. Takahashi, H. Shao, B. Zhao, W. Guo and A. W. Sandvik,  *$SO(5)$  multicriticality in two-dimensional quantum magnets* (2024), 2405.06607.

[36] H. Shao, W. Guo and A. W. Sandvik, *Quantum criticality with two length scales*, Science **352**(6282), 213 (2016), doi:[10.1126/science.aad5007](https://doi.org/10.1126/science.aad5007).

[37] S. Sachdev, *Topological order, emergent gauge fields, and Fermi surface reconstruction*, Rep. Prog. Phys. **82**(1), 014001 (2018), doi:[10.1088/1361-6633/aae110](https://doi.org/10.1088/1361-6633/aae110).

[38] H. Kageyama, K. Yoshimura, R. Stern, N. V. Mushnikov, K. Onizuka, M. Kato, K. Kosuge, C. P. Slichter, T. Goto and Y. Ueda, *Exact Dimer Ground State and Quantized Magnetization Plateaus in the Two-Dimensional Spin System  $SrCu_2(BO_3)_2$* , Phys. Rev. Lett. **82**, 3168 (1999), doi:[10.1103/PhysRevLett.82.3168](https://doi.org/10.1103/PhysRevLett.82.3168).

[39] S. Haravifard, A. Banerjee, J. van Wezel, D. M. Silevitch, A. M. dos Santos, J. C. Lang, E. Kermarrec, G. Srager, B. D. Gaulin, J. J. Molaison, H. A. Dabkowska and T. F. Rosenbaum, *Emergence of long-range order in sheets of magnetic dimers*, Proc. Natl. Acad. Sci. U.S.A. **111**(40), 14372 (2014), doi:[10.1073/pnas.1413318111](https://doi.org/10.1073/pnas.1413318111).

[40] M. E. Zayed, C. Rüegg, J. Larrea J., A. M. Läuchli, C. Panagopoulos, S. S. Saxena, M. Ellerby, D. F. McMorrow, T. Strässle, S. Klotz, G. Hamel, R. A. Sadykov *et al.*, *4-spin plaquette singlet state in the Shastry–Sutherland compound  $SrCu_2(BO_3)_2$* , Nat. Phys. **13**(10), 962 (2017), doi:[10.1038/nphys4190](https://doi.org/10.1038/nphys4190).

[41] Y. Cui, L. Liu, H. Lin, K.-H. Wu, W. Hong, X. Liu, C. Li, Z. Hu, N. Xi, S. Li, R. Yu, A. W. Sandvik *et al.*, *Proximate deconfined quantum critical point in  $SrCu_2(BO_3)_2$* , Science **380**(6650), 1179 (2023), doi:[10.1126/science.adc9487](https://doi.org/10.1126/science.adc9487).

[42] J. Guo, P. Wang, C. Huang, B.-B. Chen, W. Hong, S. Cai, J. Zhao, J. Han, X. Chen, Y. Zhou, S. Li, Q. Wu *et al.*, *Deconfined quantum critical point lost in pressurized  $SrCu_2(BO_3)_2$* , Commun. Phys. **8**(1), 75 (2025), doi:[10.1038/s42005-025-01976-8](https://doi.org/10.1038/s42005-025-01976-8).

[43] X. G. Wen, *Mean-field theory of spin-liquid states with finite energy gap and topological orders*, Phys. Rev. B **44**, 2664 (1991), doi:[10.1103/PhysRevB.44.2664](https://doi.org/10.1103/PhysRevB.44.2664).

[44] A. A. Abrikosov, *Electron scattering on magnetic impurities in metals and anomalous resistivity effects*, Physics Physique Fizika **2**, 5 (1965), doi:[10.1103/PhysicsPhysiqueFizika.2.5](https://doi.org/10.1103/PhysicsPhysiqueFizika.2.5).

[45] G. Chen, A. Essin and M. Hermele, *Majorana spin liquids and projective realization of  $SU(2)$  spin symmetry*, Phys. Rev. B **85**, 094418 (2012), doi:[10.1103/PhysRevB.85.094418](https://doi.org/10.1103/PhysRevB.85.094418).

[46] Y. Ran and X. gang Wen, *Continuous quantum phase transitions beyond Landau’s paradigm in a large- $N$  spin model* (2006), [cond-mat/0609620](https://arxiv.org/abs/cond-mat/0609620).

[47] X.-Y. Song, C. Wang, A. Vishwanath and Y.-C. He, *Unifying description of competing orders in two-dimensional quantum magnets*, Nat. Commun. **10**(1), 4254 (2019), doi:[10.1038/s41467-019-11727-3](https://doi.org/10.1038/s41467-019-11727-3).

[48] J. Alicea, *Monopole quantum numbers in the staggered flux spin liquid*, Phys. Rev. B **78**, 035126 (2008), doi:[10.1103/PhysRevB.78.035126](https://doi.org/10.1103/PhysRevB.78.035126).

[49] A. Ralko, M. Mambrini and D. Poilblanc, *Generalized quantum dimer model applied to the frustrated Heisenberg model on the square lattice: Emergence of a mixed columnar-plaquette phase*, Phys. Rev. B **80**, 184427 (2009), doi:[10.1103/PhysRevB.80.184427](https://doi.org/10.1103/PhysRevB.80.184427).

[50] P. Corboz and F. Mila, *Tensor network study of the Shastry-Sutherland model in zero magnetic field*, Phys. Rev. B **87**, 115144 (2013), doi:[10.1103/PhysRevB.87.115144](https://doi.org/10.1103/PhysRevB.87.115144).

[51] N. Xi, H. Chen, Z. Y. Xie and R. Yu, *Plaquette valence bond solid to antiferromagnet transition and deconfined quantum critical point of the Shastry-Sutherland model*, Phys. Rev. B **107**, L220408 (2023), doi:[10.1103/PhysRevB.107.L220408](https://doi.org/10.1103/PhysRevB.107.L220408).

[52] W.-Y. Liu, D. Poilblanc, S.-S. Gong, W.-Q. Chen and Z.-C. Gu, *Tensor network study of the spin- $\frac{1}{2}$  square-lattice  $J_1-J_2-J_3$  model: Incommensurate spiral order, mixed valence-bond solids, and multicritical points*, Phys. Rev. B **109**, 235116 (2024), doi:[10.1103/PhysRevB.109.235116](https://doi.org/10.1103/PhysRevB.109.235116).

[53] W.-Y. Liu, X.-T. Zhang, Z. Wang, S.-S. Gong, W.-Q. Chen and Z.-C. Gu, *Quantum Criticality with Emergent Symmetry in the Extended Shastry-Sutherland Model*, Phys. Rev. Lett. **133**, 026502 (2024), doi:[10.1103/PhysRevLett.133.026502](https://doi.org/10.1103/PhysRevLett.133.026502).

[54] X. Qian, R. Lv, J. Y. Lee and M. Qin, *From the Shastry-Sutherland model to the  $J_1-J_2$  Heisenberg model*, Phys. Rev. B **111**, L241113 (2025), doi:[10.1103/h6gc-t1wm](https://doi.org/10.1103/h6gc-t1wm).

[55] T. Senthil and M. P. A. Fisher,  *$Z_2$  gauge theory of electron fractionalization in strongly correlated systems*, Phys. Rev. B **62**, 7850 (2000), doi:[10.1103/PhysRevB.62.7850](https://doi.org/10.1103/PhysRevB.62.7850).

[56] B. Zhao, J. Takahashi and A. W. Sandvik, *Multicritical Deconfined Quantum Criticality and Lifshitz Point of a Helical Valence-Bond Phase*, Phys. Rev. Lett. **125**, 257204 (2020), doi:[10.1103/PhysRevLett.125.257204](https://doi.org/10.1103/PhysRevLett.125.257204).

[57] A. Nahum, J. T. Chalker, P. Serna, M. Ortúñoz and A. M. Somoza, *Deconfined Quantum Criticality, Scaling Violations, and Classical Loop Models*, Phys. Rev. X **5**, 041048 (2015), doi:[10.1103/PhysRevX.5.041048](https://doi.org/10.1103/PhysRevX.5.041048).

[58] A. M. Polyakov, *Gauge Fields and Strings*, vol. 3, doi:<https://doi.org/10.1201/9780203755082> (1987).

[59] R. K. Kaul and S. Sachdev, *Quantum criticality of  $U(1)$  gauge theories with fermionic and bosonic matter in two spatial dimensions*, Phys. Rev. B **77**, 155105 (2008), doi:[10.1103/PhysRevB.77.155105](https://doi.org/10.1103/PhysRevB.77.155105).

[60] A. W. Sandvik and B. Zhao, *Consistent Scaling Exponents at the Deconfined Quantum-Critical Point*, Chin. Phys. Lett. **37**(5), 057502 (2020), doi:[10.1088/0256-307x/37/5/057502](https://doi.org/10.1088/0256-307x/37/5/057502).

[61] M. S. Block, R. G. Melko and R. K. Kaul, *Fate of  $CP^{N-1}$  Fixed Points with  $q$  Monopoles*, Phys. Rev. Lett. **111**(13), 137202 (2013), doi:[10.1103/PhysRevLett.111.137202](https://doi.org/10.1103/PhysRevLett.111.137202), 1307.0519.

[62] S. M. Chester and N. Su, *Bootstrapping Deconfined Quantum Tricriticality*, Phys. Rev. Lett. **132**, 111601 (2024), doi:[10.1103/PhysRevLett.132.111601](https://doi.org/10.1103/PhysRevLett.132.111601).

[63] W.-J. Hu, F. Becca, A. Parola and S. Sorella, *Direct evidence for a gapless  $Z_2$  spin liquid by frustrating Néel antiferromagnetism*, Phys. Rev. B **88**, 060402 (2013), doi:[10.1103/PhysRevB.88.060402](https://doi.org/10.1103/PhysRevB.88.060402).

[64] M. Hering, J. Sonnenschein, Y. Iqbal and J. Reuther, *Characterization of quantum spin liquids and their spinon band structures via functional renormalization*, Phys. Rev. B **99**, 100405 (2019), doi:[10.1103/PhysRevB.99.100405](https://doi.org/10.1103/PhysRevB.99.100405).

[65] F. Ferrari and F. Becca, *Gapless spin liquid and valence-bond solid in the  $J_1$ - $J_2$  Heisenberg model on the square lattice: Insights from singlet and triplet excitations*, Phys. Rev. B **102**, 014417 (2020), doi:[10.1103/PhysRevB.102.014417](https://doi.org/10.1103/PhysRevB.102.014417).

[66] Y. Nomura and M. Imada, *Dirac-Type Nodal Spin Liquid Revealed by Refined Quantum Many-Body Solver Using Neural-Network Wave Function, Correlation Ratio, and Level Spectroscopy*, Phys. Rev. X **11**, 031034 (2021), doi:[10.1103/PhysRevX.11.031034](https://doi.org/10.1103/PhysRevX.11.031034).